Available online at www.sciencedirect.com
SCIENCE DIRECT®
Coordination Chemistry Reviews 249 (2005) 1155–1184
COORDINATION CHEMISTRY REVIEWS
www.elsevier.com/locate/ccr

Review

Structural aspects of copper catalyzed atom transfer radical polymerization

Tomislav Pintauer*, Krzysztof Matyjaszewski**

Center for Macromolecular Engineering, Department of Chemistry, Carnegie Mellon University, 4400 Fifth Avenue, Pittsburgh, PA 15213, USA

Received 28 September 2004; accepted 19 November 2004
Available online 29 December 2004

Contents

Abstract

Structural features of copper(I) and copper(II) complexes with bidentate, tridentate and tetradentate nitrogen based ligands commonly used in atom transfer radical polymerization (ATRP) were extensively reviewed and discussed based on several spectroscopic techniques. Complexing ligands included 2,2′-bipyridine (bpy), 4,4′-di(5-nonyl)-2,2′-bipyridine (dNbpy), *N*,*N*,*N*′,*N*′-tetramethylethylenediamine (TMEDA), *N*-propyl(2-pyridyl)methanimine (NPrPMI), 2,2′:6′,2″-terpyridine (tpy), 4,4′,4″-tris(5-nonyl)-

* Corresponding author. Present address: University of North Carolina at Chapel Hill, Chapel Hill, NC 27599, USA. Tel.: +1 919 962 0363; fax: +1 919 962 2476.
** Co-corresponding author. Fax: +1 412 268 6897.
E-mail addresses: tomislav@email.unc.edu (T. Pintauer), km3b@andrew.cmu.edu (K. Matyjaszewski).

0010-8545/$ – see front matter
doi:10.1016/j.ccr.2004.11.010

2,2′:6′,2″-terpyridine (tNtpy), *N*,*N*,*N*′,*N*″,*N*″-pentamethyldiethylenetriamine (PMDETA), *N*,*N*-bis(2-pyridylmethyl)octylamine (BPMOA), 1,1,4,7,10,10-hexamethyltriethylenetetramine (HMTETA), tris[2-(dimethylamino)ethyl]amine (Me_6TREN), tris[(2-pyridyl)methyl]amine (TPMA) and 1,4,8,11-tetraaza-1,4,8,11-tetramethylcyclotetradecane (Me_4CYCLAM). Additionally, structures of copper(I) and copper(II) complexes with diethylenetriamine (DETA), triethylenetetramine (TETA), *N*,*N*-bis(2-pyridylmethyl)amine (BPMA), tris[2-aminoethyl]amine (TREN) and 1,4,8,11-tetraazacyclotetradecane (CYCLAM) were discussed. The structures were found to depend on the complexing ligand, solvent and temperature.

Keywords: Atom transfer radical polymerization; Copper(I); Copper(II); Structures

1. Background

1.1. Fundamentals of atom transfer radical addition

One of the fundamental reactions in organic chemistry involves the addition of a reagent XY across a carbon–carbon double (or triple) bond through a radical process [1,2]. This reaction was first reported in the early 1940s in which the halogenated methanes were directly added to olefinic double bonds [3,4]. The process was initiated by small amounts of diacyl peroxides or by light. This reaction became known as the *atom transfer radical addition* (ATRA) *or Kharasch addition*, in honor of its discoverer, and it is generally accepted to occur via a free-radical mechanism [5,6] as illustrated in Scheme 1. However, soon after its discovery, it was realized that the use of the *Kharasch addition* reaction was rather limited because of the radical–radical coupling and repeating radical addition to olefin to generate oligomers and polymers. Although the radical–radical coupling could be suppressed by decreasing the radical concentration, telomerization reactions could not be avoided due to the low chain transfer constant, k_{tr}/k_p. The research was thus shifted in a direction of finding means to selectively control the product distribution.

In 1960s, several groups began to investigate the use of transition metal complexes to catalyze the ATRA. The basic idea to enhance the chemoselectivity of the mono halogenated product was to increase the chain transfer constant, k_{tr}/k_p (Scheme 1). This was achieved by recognizing that the transition metal complexes are much more effective halogen transfer agents than alkyl halides. A number of species were found to be particularly effective and they included the complexes of Cu [7–10], Fe [10–13], Ru [14,15] and Ni [16,17]. These also included the use of metal oxides [18,19] or zero valent metals such as Cu(0) [20,21] or Fe(0) [22–24]. Great progress has been made in not just controlling the product selectivity, but also in utilizing a variety of halogenated compounds (alkyl and aryl halides [25–27], *N*-chloroamines [27], alkylsulfonyl halides [28–33], and polyhalogenated compounds [10,13,34,35]). Furthermore, it was also demonstrated that a variety of olefins (styrene, alkyl acrylates and acrylonitrile) could be used as the source of reactive unsaturation. Thus, the transition metal catalyzed (TMC) ATRA became broadly applicable synthetic tool [36–39].

The mechanism of the transition metal catalyzed ATRA has been extensively studied. Although there is still an ongoing argument on the nature of the reactive intermediates, the generally accepted mechanism (Scheme 2) [27,40], which applies to the majority of the transition metal complexes, involves radical intermediates. Homolytic cleavage of the alkyl halide bond (R–X) by the transition metal complex in the lower oxidation state generates an alkyl radical $R^{\bullet}$ and the corresponding transition metal complex in the higher oxidation state. The radical $R^{\bullet}$ adds across the double bond of an olefin, terminates by radical coupling and disproportionation, or abstracts the halogen from the transition metal complex in the higher oxidation state. The key to increase the chemoselectivity of the mono-halogenated adduct lies in the radical generating step. In order to achieve that, the following general guidelines need to be met:

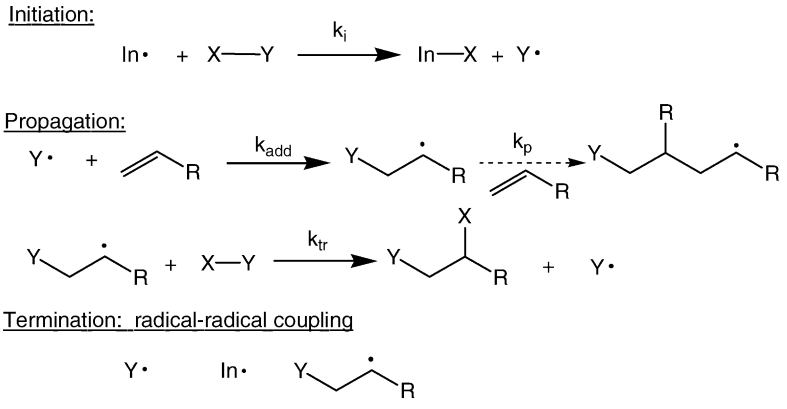

Scheme 1. Mechanism of the free-radical addition to olefins.

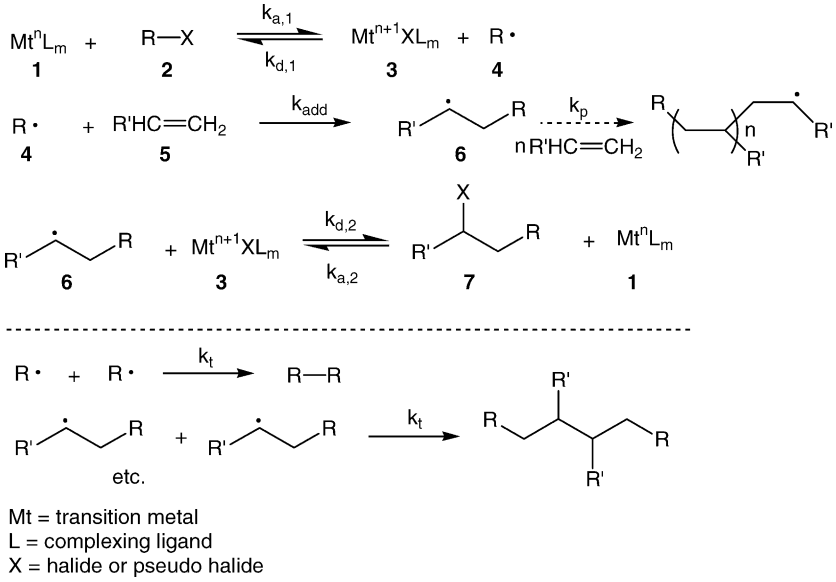

Scheme 2. Proposed mechanism for the transition metal catalyzed ATRA.

(1) Rate of activation ($k_{a,1}$ and $k_{a,2}$) ≪ rate of deactivation ($k_{d,1}$ and $k_{d,2}$); this is required in order to maintain low radical concentration and suppress radical termination reactions.
(2) $k_{a,1} \gg k_{a,2}$: the generation of the radical **4** from **2** should be faster than that from the product **7** in order to avoid further formation of radical **6** which continuously adds to the alkenes and leads to oligomeric/polymeric species.
(3) Rate of transfer ≫ rate of propagation ($k_{d,2}$[$Mt^{n+1}XL_m$, **3**] ≫ k_p[alkene, **5**]); after the addition of radical **4** to alkene **5**, the atom transfer to the adduct **7** should occur before the addition to the monomer molecules.

1.2. Fundamentals of atom transfer radical polymerization

Over the past few years, we have witnessed a tremendous development of controlled radical polymerization techniques for the synthesis of macromolecules with well-defined compositions, architectures and functionalities [41–44]. Particularly, atom transfer radical polymerization (ATRP) has gained a considerable academic and industrial interest [42,43,45–47]. Similarly to transition metal catalyzed ATRA, ATRP also employs transition metal complexes as halogen transfer agents. A general mechanism for ATRP is shown in Scheme 3 [48–59]. Homolytic cleavage of the alkyl (pseudo)halogen bond (R–X) by a transition metal complex in the lower oxidation state (Mt^n–Y/ligand) generates an alkyl radical (R•) and a transition metal complex in the higher oxidation state (X–Mt^{n+1}–Y/ligand). The formed radicals can initiate the polymerization by adding across the double bond of a vinyl monomer, propagate, terminate by either coupling or disproportionation, or be reversibly deactivated by the transition metal complex in the higher oxidation state. The formation of radicals during the ATRP process is reversible.

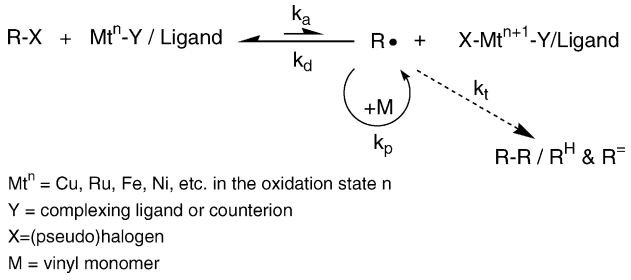

Scheme 3. Transition metal catalyzed ATRP.

Furthermore, their stationary concentration is low because the equilibrium between the activation (k_a) and deactivation (k_d) processes is shifted to the left-hand side (i.e. $k_a \ll k_d$), which reduces the termination reactions. As a result of persistent radical effect [60,61], polymers with predictable molecular weights, narrow molecular weight distributions and high functionalities have been synthesized [62–84].

So far, in ATRP, a variety of transition metal complexes have been successfully used for the polymerization of styrenes [85–87], (meth)acrylates [88–100], acrylonitriles [101–103], and acrylamides [104–106]. They include compounds from Groups 4 (Ti [107]), 6 (Mo [108,109]), 7 (Re [110]), 8 (Fe [111–116], Ru [117]), 9 (Rh [118]), 10 (Ni [119], Pd [120]) and 11 (Cu [47,85,121–131]). Typical ATRP initiators are alkyl halides, including halogenated alkanes [47,84,117,119,122,132], α-haloesters [89,133–135] and sulfonyl chlorides [136–138].

2. Introduction

As indicated in the previous section, one of the principal components of the TMC ATRA and ATRP systems involves

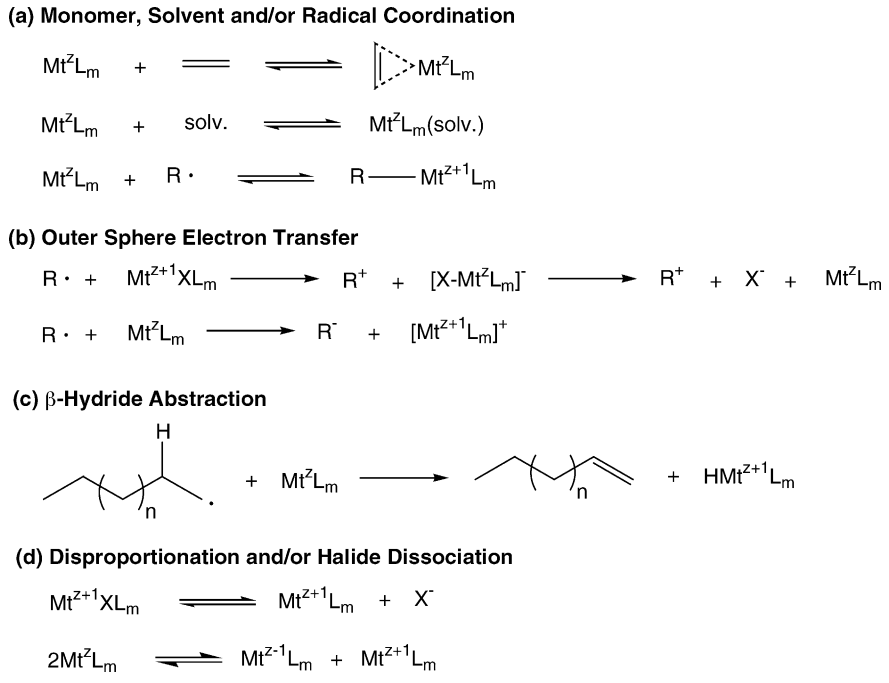

Scheme 4. Possible side reactions in metal catalyzed ATRP/ATRP.

the transition metal complex, which is used as a halogen transfer agent. Perhaps, it is the most important component of both systems since it determines the position of the atom transfer equilibrium and the dynamics of exchange between the dormant and active species. Consequently, structural characterization of the ATRA/ATRP active transition metal complexes plays an important role in the overall catalytic process. The catalyst typically consists of a transition metal center accompanied by a complexing ligand and counter-ion which can form a covalent or ionic bond with the metal center. An efficient catalyst should be able to expand its coordination sphere and oxidation number upon halogen abstraction from alkyl halide or dormant polymer chains. Additionally, the catalyst should not participate in any side

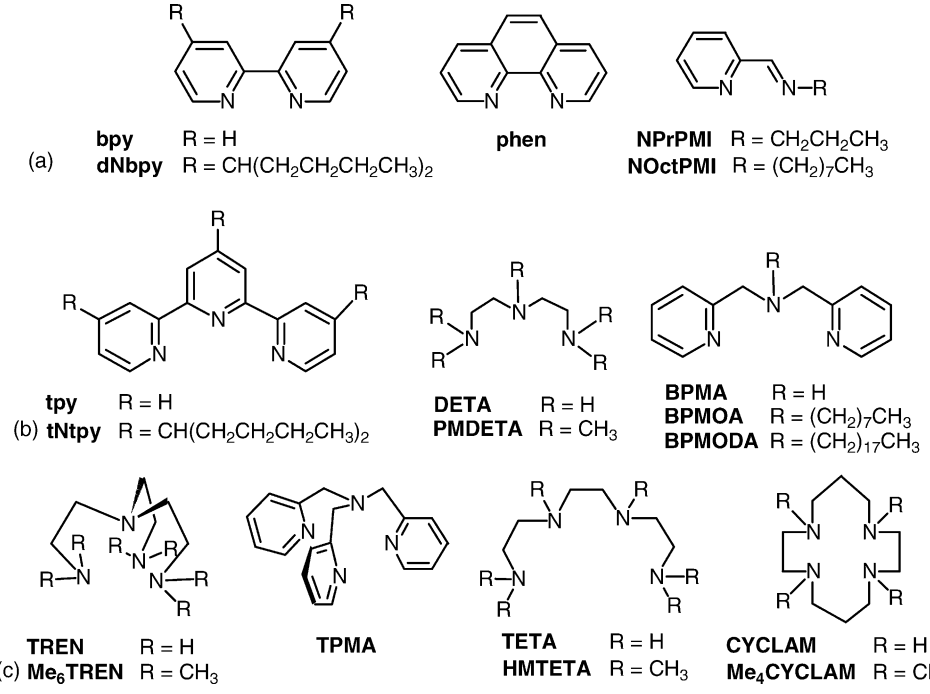

Scheme 5. Structures of bidentate (a), tridentate (b) and tetradentate (c) nitrogen based ligands commonly used in copper catalyzed ATRP.

reactions which would lower its activity or change the radical nature of the ATRA/ATRP process. The concurrent reactions which can occur during the catalytic process include: (a) monomer, solvent or radical coordination, (b) oxidation/reduction of radicals to radical cations/anions, respectively, (c) β-hydrogen abstraction, (d) disproportionation, etc. (Scheme 4). In ATRP, so far, a variety of transition metal complexes have been successfully used. They include compounds from Groups 4 (Ti [107]), 6 (Mo [108,109]), 7 (Re [110]), 8 (Fe [111–116], Ru [117]), 9 (Rh [118]), 10 (Ni [119], Pd [120]) and 11 (Cu [47,85,121–131]). The following review will concentrate on the structural features of copper(I) and copper(II) complexes with nitrogen based ligands that are commonly used for ATRP (Scheme 5). They include 2,2′-bipyridine (bpy) [47], 4,4′-di(5-nonyl)-2,2′-bipyridine (dNbpy) [49,85], 1,10-phenanthroline (phen) [139], *N*,*N*,*N*′,*N*′-tetramethylethylenediamine (TMEDA) [140,141], *N*-propyl-(2-pyridyl)methanimine (NPrPMI), 2,2′:6′,2″-terpyridine (tpy) [142], 4,4′,4″-tris(5-nonyl)-2,2′:6′,2″-terpyridine (tNtpy) [142], *N*,*N*,*N*′,*N*″,*N*″-pentamethyldiethylenetriamine (PMDETA) [143], *N*,*N*-bis(2-pyridylmethyl)octylamine (BPMOA) [130], 1,1,4,7,10,10-hexamethyltriethylenetetramine (HMTETA) [140,144], tris[2-(dimethylamino)ethyl]amine (Me_6TREN) [145], tris[(2-pyridyl)methyl]amine (TPMA) [131] and 1,4,8,11-tetraaza-1,4,8,11-tetramethylcyclotetradecane (Me_4CYCLAM) [106]. Additionally, we will also discuss structures of copper(I) and copper(II) complexes with diethylenetriamine (DETA), triethylenetetramine (TETA), *N*,*N*-bis(2-pyridylmethyl)amine (BPMA), tris[2-aminoethyl]amine (TREN) and 1,4,8,11-tetraazacyclotetradecane (CYCLAM). A detailed discussion of structural chemistry of copper complexes with other nitrogen based ligands, including sulfur, phosphorous and oxygen based ligands, has been reviewed extensively in other literature sources [146–149].

3. Copper(I) complexes with nitrogen based ligands

3.1. Bidentate ligands

3.1.1. bpy and bpy derivatives

3.1.1.1. Solid state studies. Copper(I) complexes with bpy based ligands (bpy) are typically prepared by mixing Cu^IY or its complex with CH_3CN (Y = Br^-, Cl^-, PF_6^-, ClO_4^-, BF_4^-, etc.) with 2 eq. of the ligand, and can generally be represented by the following formula $[Cu^I(bpy)_2]^+[Y]^-$. Additionally, in the case of Cu^IBr and Cu^ICl salts, the corresponding Y can also be $[Cu^IBr_2]^-$ and $[Cu^ICl_2]^-$ anion, respectively. In the solid state, $[Cu^I(bpy)_2]^+$ cations are typically distorted tetrahedral in geometry (Fig. 1) in which the copper(I) center is coordinated by four nitrogen atoms from two bpy units [150]. The average Cu^I–N bond lengths and intraligand N–Cu^I–N angles for a series of $[Cu^I(bpy)_2]^+[Y]^-$ complexes are summarized in Table 1

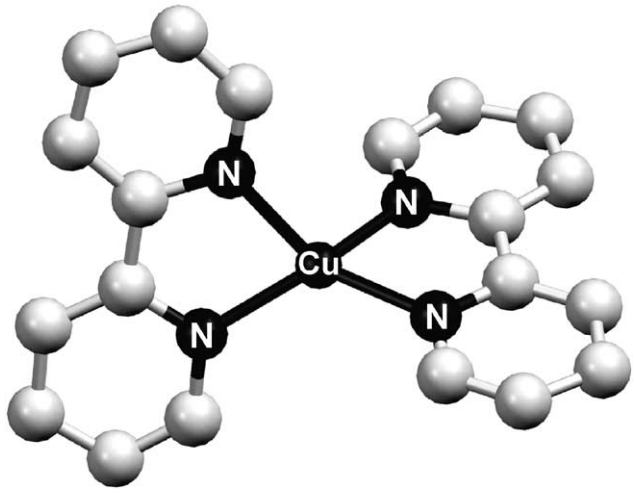

Fig. 1. Structure of $[Cu^I(bpy)_2]^+$ cation in $[Cu^I(bpy)_2]^+[ClO_4]^-$ [150].

[150–155]. The average Cu^I–N bond length ranges from 1.985 to 2.057 Å and is not greatly affected by either the counter-ion or the substituent on the bpy ligand. Furthermore, the "bite" angles are restricted to 80–83° range by the rigid geometry of the bidentate bipyridine based ligand. However, as indicated in Table 1, the dihedral angles between the CuN_2 planes show a wide variation. The smallest dihedral angle was observed in $[Cu^I(bpy)_2]^+[PF_6]^-$ complex (44.6°) and the largest one in $[Cu^I(dNEObpy)_2]^+[Cu^IBr_2]^-$ (89.0°), which is also an effective catalyst in the ATRP (Fig. 2) [155]. The differences in dihedral angles can mostly be attributed to crystal packing forces as discussed in literature [156,157]. Consequently, the relatively large dihedral angle in $[Cu^I(dNEObpy)_2]^+[Cu^IBr_2]^-$ complex is induced by the large side chains occupying space between the bis(bipyridine)copper(I) cores [155]. It has also been observed that dihedral angle affects the redox potential of $[Cu^I(bpy)_2]^+$ cation, and consequently the stability constants of $[Cu^I(bpy)_2]^+$ and $[Cu^{II}(bpy)^2]^{2+}$ cations [150]. Generally, 6,6′-substitution increases a redox potential. For example, $E_{1/2}$ (versus NHE) for $[Cu^I(bpy)_2][ClO_4]^-$ (dihedral an-

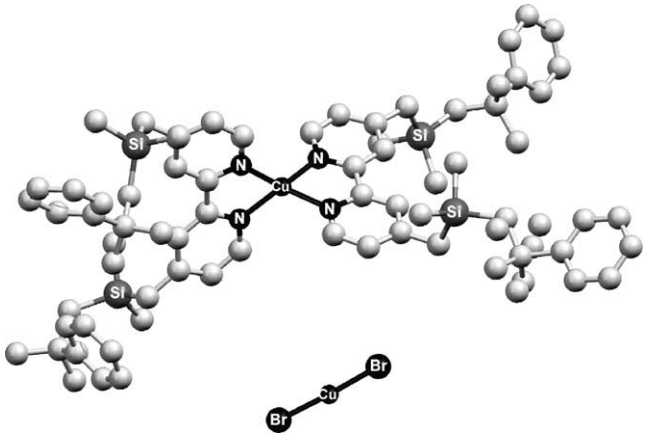

Fig. 2. Molecular structure of $[Cu^I(dNEObpy)_2]^+[Cu^IBr_2]^-$ [155].

Table 1
Comparison of structural parameters for some $[Cu^{I}(bpy)_2]^{+}[Y]^{-}$ complexes

bpy[a]	Y	Cu^{I}—N_{AV} (Å)[b]	N—Cu^{I}—N_{AV} (°)[b]	Dihedral angle[c]	Reference
bpy	ClO_4^-	2.021	81.5	75.2	[150]
	PF_6^-	1.985	83.0	44.6	[151]
	$Cu^{I}Cl_2^-$	2.022	81.2	76.2	[152]
4,4′-dmbpy	Br^-	2.047	80.7	54.2	[153]
6,6′-dmbpy	BF_4^-	2.034	81.9	80.7	[154]
4,4′,6,6′-tmbpy	ClO_4^-	2.057	80.6	68.1	[151]
dNEObpy	$Cu^{I}Br_2^-$	2.035	81.4	89.0	[155]

[a] bpy = 2,2′-bipyridine; 4,4′-dmbpy = 4,4′-dimethyl-2,2′-bipyridine; 6,6′-dmbpy = 6,6′-dimethyl-2,2′-bipyridine; 4,4′,6,6′-dtmbpy = 4,4′,6,6′-tetramethyl-2,2′-bipyridine; dNEObpy = 4,4′-bis(neophyldimethylsilylmethyl)-2,2′-bipyridine.
[b] Bond lengths and intraligand N—Cu—N angle, two values are averaged.
[c] Interligand dihedral angle.

Table 2
Bond lengths and angles in $[Cu^{I}Br_2]^-$ and $[Cu^{I}Cl_2]^-$ anions

Complex	Cu^{I}—X_1 (Å)	Cu^{I}—X_2 (Å)	X_1—Cu^{I}—X_2 (°)	Reference
$[Cu^{I}(dNEObpy)_2]^{+}[Cu^{I}Br_2]^-$	2.223(2)	2.234(3)	177.4	[155]
$[N(C_4H_9)_4]^{+}[Cu^{I}Br_2]^-$	2.226(1)	2.226(1)	180.0	[159]
$[P(C_6H_5)_4]^{+}[Cu^{I}Br_2]^-$	2.211(2)	2.216(2)	174.6	[160]
$[Cu^{I}(bpy)_2]^{+}[Cu^{I}Cl_2]^-$	2.086(2)	2.091(2)	177.3	[152]
$[N(C_4H_9)_4][Cu^{I}Cl_2]^-$	2.094(2)	2.092(2)	179.2	[159]

gle = 75.2°) is 0.254 V [150], whereas the $E_{1/2}$ (versus NHE) for $[Cu^{I}(6,6'\text{-dmbpy})_2]^{+}[BF4]^-$ (dihedral angle = 80.7°) is significantly higher, 0.574 V [150,158].

As indicated in Table 1, for $Cu^{I}Cl$ and $Cu^{I}Br$ complexes with bpy ligand, the stoichiometry can sometimes be 1:1, resulting in the formation of $[Cu^{I}Br_2]^-$ and $[Cu^{I}Cl_2]^-$ anions. Table 2 compares the bond lengths and angles in $[Cu^{I}(bpy)_2]^{+}[Cu^{I}Cl_2]^-$ and $[Cu^{I}(dNEObpy)_2]^{+}[Cu^{I}Br_2]^-$ with a series of model compounds with $[Cu^{I}Br_2]^-$ and $[Cu^{I}Cl_2]^-$ anions [152,155,159,160]. As evident from Table 2, $[Cu^{I}Br_2]^-$ and $[Cu^{I}Cl_2]^-$ bond lengths and angles in $[Cu^{I}(dNEObpy)_2]^{+}[Cu^{I}Br_2]^-$ and $[Cu^{I}(bpy)_2]^{+}[Cu^{I}Cl_2]^-$, respectively, do not change significantly when compared with model compounds, indicating insignificant interactions with Cu^{I} cations.

With respect to $Cu^{I}X$ (X = halide) complexes with bpy based ligands, an additional mode of coordination was observed which includes the formation of Cu–X bridged complexes. This has been demonstrated in the isolation and X-ray structure determination of $[Cu^{I}(bpy)Br]_2$ and $[Cu^{I}(bpy)I]_2$ dimers (Fig. 3) [152]. In $[Cu^{I}(bpy)Br]_2$, each Cu^{I} center has distorted tetrahedral geometry and is coordinated by two nitrogen atoms of a bipyridine ligand (Cu^{I}–N = 2.083(6) and 2.099(5) Å) and two bromide ions (Cu^{I}–Br = 2.428(2) and 2.463(1) Å). The distance between the two Cu^{I} centers was determined to be 2.850(1) Å. The structure of $[Cu^{I}(bpy)I]_2$ dimer was analogous to $[Cu^{I}(bpy)Br]_2$ (Cu^{I}–N = 2.070(8) and 2.080(1) Å, Cu^{I}–I = 2.583(3) and 2.587(4) Å, Cu^{I}–Cu^{I} = 2.610(2) Å).

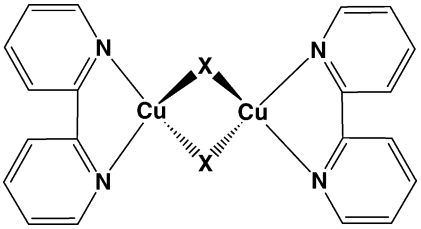

Fig. 3. Structure of $[Cu^{I}(bpy)X]_2$ (X = Br and I) dimer.

3.1.1.2. Solution studies. The discussion in the previous section has extensively focused on the characterization of Cu^{I} complexes with bpy based ligands in the solid state. The structures might not be fully correct in solution, particularly taking into account the possibility that more than one species coexist in an equilibrium. A variety of other experimental techniques have been used to probe the structures of Cu^{I} complexes with bpy based ligands in solution and are summarized below.

Far IR and Raman spectroscopy: The coordination of halogens to Cu^{I} complexes has been extensively studied by far IR spectroscopy [161–163], particularly, $[Cu^{I}Br_2]^-$ anions which are sometimes present as counter-ions in $Cu^{I}Br$/2bpy systems, as discussed above. They have linear geometry and belong to $D_{\infty h}$ point group. According to a normal mode analysis, they should have one Raman active band ($\upsilon_1(\Sigma_g^{+})$) and two IR active bands ($\upsilon_2(\Pi_u)$ and $\upsilon_3(\Sigma_u^{+})$). It was found experimentally that the Raman active band for a series of Cu^{I} complexes with $[Cu^{I}Br_2]^-$ anions appears around 192–194 cm^{-1}. On the other hand, IR active bands appear at 73–81 and 320–322 cm^{-1} [162,163]. Furthermore, the coordination of bpy based ligands to the Cu^{I} center has also been investigated. For tetrahedral $[Cu^{I}(bpy)_2]^{+}$ cations, Cu^{I}–N vibrational stretches typically appear around 300 cm^{-1} [164–169].

Table 3
Absorption maxima and extinction coefficients for Cu^I complexes with bpy

Complex	Solvent	λ_{max} (nm)	ε_{max} (M^{-1} cm^{-1})
$[Cu^I(bpy)Cl]_2$	Acetone	440	2400
$[Cu^I(bpy)Br]_2$	Acetone	440	2400
$[Cu^I(bpy)I]_2$	Acetone	436	1600
$[Cu^I(bpy)_2]^+[Cl]^-$	Ethanol	440	3800
$[Cu^I(bpy)_2]^+[Br]^-$	Ethanol	440	3900
$[Cu^I(bpy)_2]^+[ClO_4]^-$	Acetone	440	4800
$[Cu^I(bpy)_2]^+[ClO_4]^-$	Ethanol	440	5400

UV–vis spectroscopy: UV–vis spectroscopy was also used to investigate structural features of Cu^I complexes with bpy ligands in solution. Typically, Cu^I complexes with bpy ligands are dominated by intense broad absorption bands with maxima at a wavelength in the range 440–470 nm [170]. This absorption was assigned by Irving and Williams [171] as a metal to ligand charge transfer (MLCT) transition wherein an electron is promoted from a 3d orbital of copper to a low lying π^* orbital of the bpy ligand. Some studies have suggested that the intensity of this MLCT transition should be proportional to the number of bpy units coordinated to the Cu^I center [172–175]. It was found that the extinction coefficients for a series of Cu^IX (X = Br, Cl and I) complexes with bpy in non-polar medium such as acetone are approximately half the values in polar medium such as ethanol and for Cu^I/bpy complexes with non-coordinating anions (Table 3) [176]. Based on these results, it was proposed that in non-polar medium Cu^IX complexes with bpy predominantly exist as bridged $[Cu^I(bpy)X]_2$ species (see Fig. 3). In polar medium, on the other hand, the predominant complexes are $[Cu^I(bpy)_2]^+[X]^-$. However, the two-fold decrease in the extinction coefficient in non-polar medium can alternatively be explained by the formation of $[Cu^I(bpy)_2]^+[Cu^IX_2]^-$ complexes, as discussed above.

^{1}H NMR spectroscopy: Levy et al. have investigated the solution behavior of an isolated and structurally characterized ATRP active $[Cu^I(dNEObpy)_2]^+[Cu^IBr_2]^-$ (dNEObpy = 4,4′-bis(neophyldimethylsilylmethyl)-2,2′-bipyridine) complex in polar and non-polar medium by ^{1}H NMR [155]. Based on their results, they proposed that in non-polar medium the complex predominantly exist as $[Cu^I(dNEObpy)_2]^+[Cu^IBr_2]^-$. In polar medium, on the other hand, $[Cu^I(dNEObpy)_2]^+[Br]^-$ is preferred (Scheme 6). Consequently, their findings indicated that 1:1 stoichiometry between Cu^IBr and dNEObpy can be used in non-polar medium, including monomers that are typically polymerized by ATRP.

Electrospray ionization mass spectrometry (ESI-MS): Since the report of the first coordination complex detected by electrospray ionization mass spectrometry (ESI-MS) in 1990 [177], coordination chemistry studies by ESI-MS have developed substantially [178–181]. One of the main advantages of this method lies in the fact that it provides information about positively and negatively charged species present in solution by observing them in the gas phase. This is achieved by aerosolizing the solution while concomitantly applying a static charge to the surface of solvent droplets. $[Cu^I(bpy)_2]^+[BF_4]^-$ complex has been studied by ESI-MS in methanol [182]. The positive and negative ion spectra indicated the presence of only $[Cu^I(bpy)_2]^+$ cations and $[BF_4]^-$ anions, respectively, which was consistent with the solid state X-ray structure of the complex [154]. Furthermore, mass spectra of Cu^IBr complexed with one or two equivalents of 4,4′-di(5-nonyl)-2,2′-bipyridine (dNbpy) in toluene (Fig. 4), methyl acrylate or styrene showed the presence of $[Cu^I(dNbpy)_2]^+$ cation and $[Cu^IBr_2]^-$ anion [183]. This result indicated that in non-polar medium the stoichiometry between Cu^IBr and dNbpy is 1:1, as opposed to 1:2 typically observed in polar medium.

Extended X-ray absorption fine structure (EXAFS): Extended X-ray absorption fine structure (EXAFS) spectroscopy has been known since early 1930 [184–186], however, its full potential in determining the structures of transition metal complexes has not been utilized until early 1970s [187]. This was particularly due to the unavailability of strong X-ray sources. With the development of synchrotron radiation, EXAFS has been established as a practical structural tool [188–190]. The EXAFS measurements provide information on the bond length, the coordination number and the nature of the scattering atoms surrounding an excited atom [191]. Since EXAFS is mostly sensitive to short-range ordering, it can be used to study immediate environment around each absorber (generally out to ∼4 Å). Other materials or im-

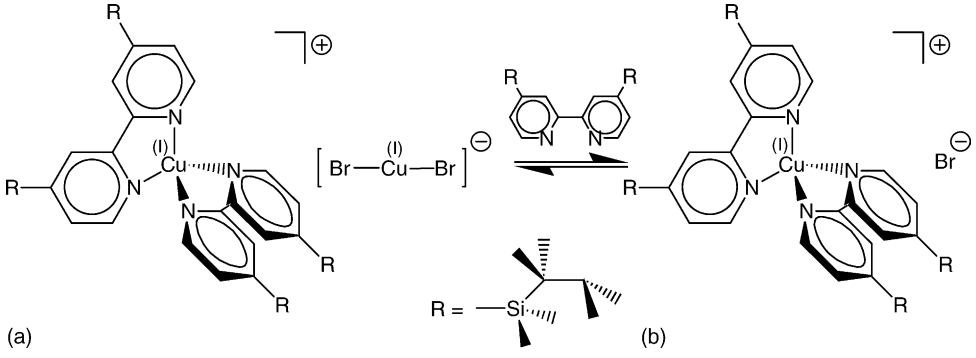

Scheme 6. Proposed structures for Cu^IBr/2dNEObpy complex in non-polar (a) and polar (b) medium.

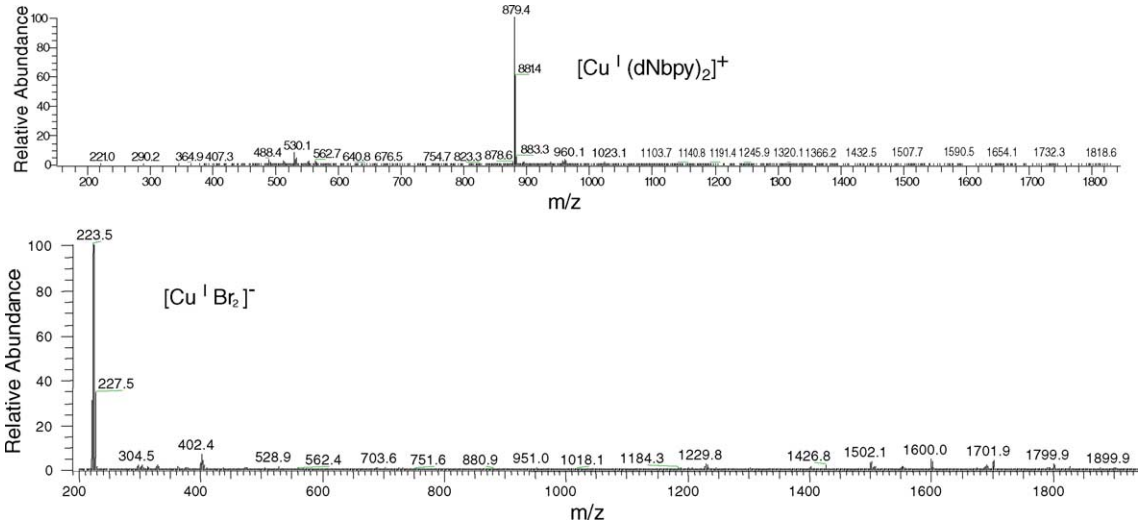

Fig. 4. Mass spectra of $Cu^{I}Br$/2dNbpy in toluene (positive and negative ion modes).

purities present in the sample which either do not contain the absorber or are far from the absorber will not interfere. Furthermore, it is highly versatile in that it can be applied with high accuracy (0.01–0.03 Å) to matter in the solid (crystalline or amorphous), liquid, solution, or gaseous state [192].

Table 4 shows the summary of room temperature EXAFS measurements of $Cu^{I}Br$ complex with dNbpy ligand in methyl acrylate and styrene, which are typical monomers used in the ATRP [193–195]. The EXAFS spectrum of $Cu^{I}Br$ complex with 1 eq. of dNbpy ligand in styrene is well fit assuming that Cu^{I} is coordinated by on average 3.8 nitrogen atoms at the distance of 2.01 Å and 1.1 bromine atoms at the distance of 2.25 Å. The results in methyl acrylate are analogous, indicating similar structural features of the complex. Furthermore, when 2 eq. of dNbpy ligand were used relative to $Cu^{I}Br$, the average Cu^{I}–N and Cu^{I}–Br distances did not change significantly, although the coordination number of nitrogen appears to be lower than in solutions that contained only 1 eq. of dNbpy ligand. Taking into account the inherent error of 10–15% for the coordination numbers, one possible structure in non-polar medium is ionic $[Cu^{I}(dNbpy)_2]^{+}[Cu^{I}Br_2]^{-}$ complex. Fig. 5 shows the Fourier transforms of the EXAFS functions at the Br K-edge of $Cu^{I}Br$/2dNbpy complex in toluene and $[N(C_4H_9)_4]^{+}[Cu^{I}Br_2]^{-}$ in the solid state. The similarity of the two spectra further suggested the presence of $[Cu^{I}Br_2]^{-}$ anions in $Cu^{I}Br$/2dNbpy complex in non-polar medium, which is consistent with the proposed $[Cu^{I}(dNbpy)_2]^{+}[Cu^{I}Br_2]^{-}$ complex.

Since EXAFS represents the average structure, $[Cu^{I}(dNbpy)_2]^{+}[Cu^{I}Br_2]^{-}$ might not be the only complex present in solution, taking into account the possibility for more than one species coexisting in an equilibrium. Depending on the temperature, solvent polarity, and the

Table 4
Structural parameters of $Cu^{I}Br$ complex with dNbpy ligand, determined by EXAFS measurements under ambient conditions at the Cu K- and Br K-edge

Solvent	Backscattering	N	r (Å)	σ (Å)	ΔE_0 (eV)	k (Å^{-1})	Fit index
$Cu^{I}Br$:dNbpy = 1:1							
Styrene	Cu—N	3.8	2.01	0.096	18.7	3.8–12.5	27.6
	Cu—Br	1.1	2.25	0.078			
	Br—Cu	0.8	2.24	0.074	21.8	4.1–12.6	27.8
MA	Cu—N	3.7	1.99	0.100	13.6	4.0–12.5	29.6
	Cu—Br	1.3	2.26	0.090			
	Br—Cu	1.0	2.26	0.100	18.5	4.3–12.0	19.6
$Cu^{I}Br$:dNbpy = 1:2							
Styrene	Cu—N	2.9	2.03	0.105	19.0	4.1–12.0	36.2
	Cu—Br	1.4	2.25	0.105			
	Br—Cu	0.8	2.24	0.087	21.2	4.3–12.5	29.6
MA	Cu—N	2.8	2.01	0.100	21.9	4.2–12.5	20.7
	Cu—Br	1.3	2.26	0.090			
	Br—Cu	0.8	2.25	0.100	14.5	4.2–12.0	34.5

N: coordination number, r: absorber–backscatterer distance, σ: Debye–Waller factor. Inherent errors are 10–15% for coordination numbers and Debye–Waller factors and 1% for distances.

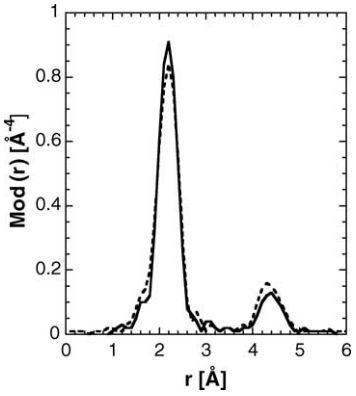

Fig. 5. Comparison of the experimental Fourier transformed $k^3\chi(k)$ functions at the Br K-edge of Cu^IBr/dNbpy in toluene (solid line) and $[N(C_4H_9)_4][Cu^IBr_2]$ in the solid state (broken lines).

amount of dNbpy ligand, the substitution of bromine in $[Cu^IBr_2]^-$ by dNbpy ligand may lead to the formation of $[Cu^I(dNbpy)_2]^+[Br]^-$. A similar equilibrium has been proposed earlier for $[Cu^I(dNEObpy)_2]^+[Cu^IBr_2]^-$ complex (Scheme 6) [155]. Also, on the other hand, solvent and monomer coordination to the Cu^I center [196] cannot be ruled out due to the sensitivity of EXAFS measurements [197].

3.1.1.3. Substitution reactions. Bipyridine based ligands (bpy) are typically rapidly exchanging in solution when complexed to copper(I) center, therefore increasing the possibility for ligand substitution reactions. In the simplest case, the bpy ligand can be substituted by coordinating solvent as demonstrated in the case of $[Cu^I(bpy)(CH_3CN)_2]^+[ClO_4]^-$ complex [198]. In the case of ATRA and ATRP processes, the bpy ligand can be substituted by monomer, which is typically present in a large excess relative to the Cu^I complex. Monomer coordination has been demonstrated by the isolation and characterization of $[Cu^I(bpy)(\pi\text{-}CH_2CH(C_6H_5))]^+[ClO_4]^-$ complex [196]. The Cu^I center in the complex is coordinated by two nitrogen atoms of a bpy ligand, one oxygen atom from the ClO_4^- anion, and the pseudotetrahedral geometry is completed by a π-interaction with the double bond of styrene. The vinyl protons of coordinated styrene are shielded relative to free styrene indicating the presence of π-back donation from the electron rich Cu^I. Additionally, Cu^I/bpy complexes with ethylene, propylene, and series of other olefins with the general formula $[Cu^I(bpy)(\pi\text{-olefin})]^+[ClO_4]^-$ have been reported [198,199].

Copper(I) complexes with 1,10-phenanthroline ligand are expected to show coordination behavior similar to bpy and bpy derivatives discussed above.

3.1.2. N-Alkyl(2-pyridyl)methanimine ligands

Chelating bis(imine) ligands such as *N*-alkyl(2-pyridyl)methanimine (AlkPMI) ligands have also been successfully used in copper mediated ATRP [121,200–208]. In particular, complexes $[Cu^I(n\text{-PrPMI})_2]^+[PF_6]^-$, $[Cu^I(i\text{-BuPMI})_2]^+[BF_4]^-$ and $[Cu^I(sec\text{-BuPMI})_2]^+[BF_4]^-$ have been isolated and structurally characterized (Fig. 6) [201]. In all three complexes, copper(I) centers are distorted tetrahedral in geometry with the average Cu^I–N bond lengths (2.019 Å (*n*-Pr), 2.037 Å (*i*-Bu) and 2.087 Å (*sec*-Bu)), N–Cu–N angles (80.75° (*n*-Pr), 81.09° (*i*-Bu) and 81.12° (*sec*-Bu)) and dihedral angles (85.3° (*n*-Pr), 86.8° (*i*-Bu) and 86.2° (*sec*-Bu)) similar to bpy derivatives (Table 2). This similarity in the solid state structures between Cu^I/AlkPMI and Cu^I/bpy complexes is also reflected in their comparable ATRP activity [209]. However, these two classes of complexes might undergo different side reactions in solution such as loss of ligand, monomer and/or solvent coordination and halide anion dissociation. Monomer coordination has been demonstrated in the case of ATRP of aminoethyl methacrylates and methoxy[poly(ethylene glycol)]methacrylates catalyzed by Cu^IBr/2*n*-PrPMI complex [203].

3.1.3. TMEDA

N,*N*,*N*′,*N*′-Tetramethylethylenediamine (TMEDA) is inexpensive bidentate aliphatic nitrogen based ligand which was successfully used in ATRP of styrene, methyl acrylate and 2-(dimethylamino)ethyl methacrylate [140,141]. Typically, 2 eq. of TMEDA relative to Cu^IBr were used in the polymerization and the activity of the catalyst was generally lower when compared to bpy and its derivatives.

Several copper(I) complexes with TMEDA ligand have been isolated and characterized. Crystal structure of $[Cu^I(TMEDA)_2]^+[BPh_4]^-$ indicated that copper(I) cation is nearly tetrahedral with the dihedral angle of 86.1° and average Cu–N bond length of 2.210 Å [210]. Similar structural features were also observed in $[Cu^I(TMEDA)_2]^+[Cu^ICl_2]^-$

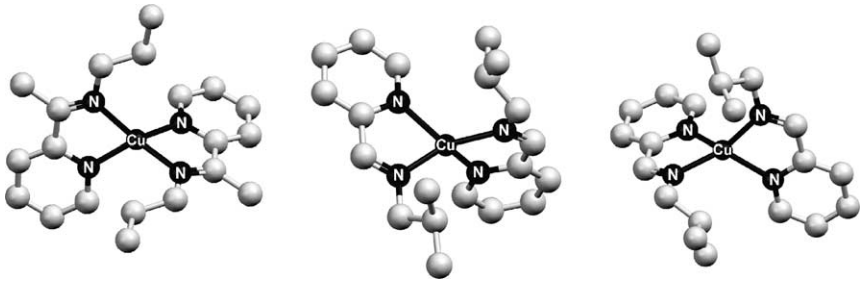

Fig. 6. Structures of $Cu^I(PrPMI)_2^+$, $Cu^I(i\text{-BuPMI})_2^+$ and $Cu^I(sec\text{-BuPMI})_2^+$ cations.

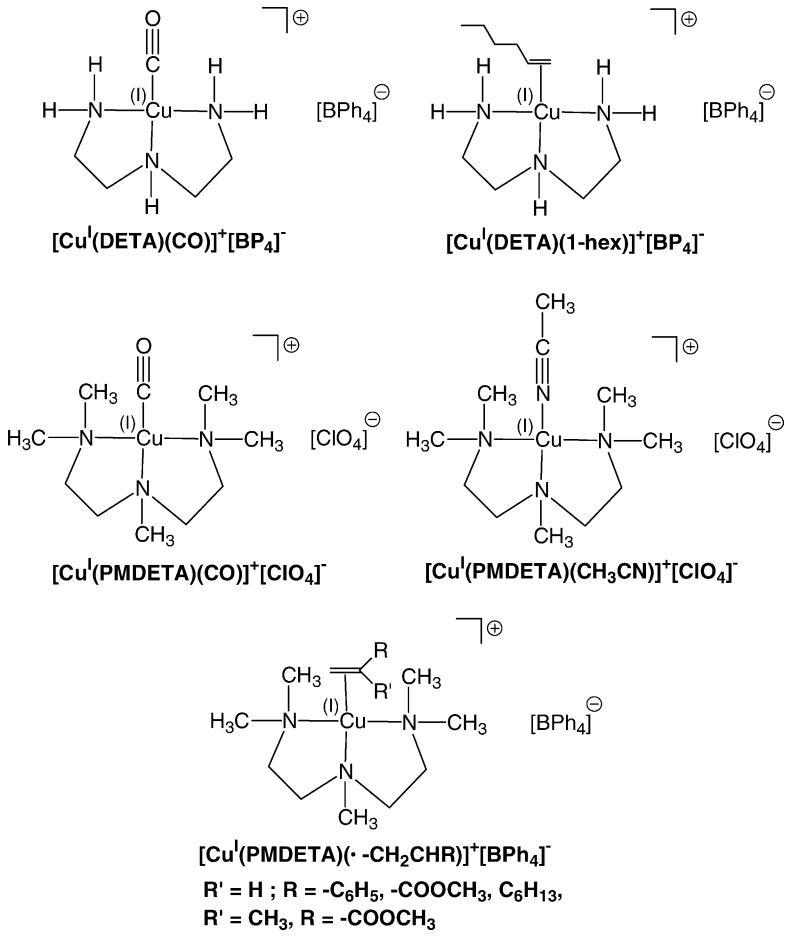

Scheme 7. Structures of Cu^I complexes with DETA and PMDETA ligands.

complex which was isolated by reaction of Cu^ICl with 1 eq. of TMEDA ligand [211,212]. $[Cu^ICl_2]^-$ anion was found to be linear with Cu^I–Cl bond length of 2.086 Å. This 1:1 stoichiometry between Cu^I and TMEDA has also been observed in the case of Cu^IBr and Cu^II. However, the latter salts predominantly formed $[Cu^I(TMEDA)Br]_2$ and $[Cu^I(TMEDA)I]_2$ dimers [211].

3.2. Tridentate ligands

3.2.1. DETA and PMDETA

Apart from substituted bipyridines, other linear and cyclic amines were successfully used as ligands for ATRP catalysts [140,143,145,213]. Particularly, commercially available tridentate *N*,*N*,*N*′,*N*″,*N*″-pentamethyldiethylenetriamine (PMDETA) showed a high potential for the controlled polymerization of a variety of monomers. Typically, the ligand to copper(I) halide ratio used in the polymerization was 1:1.

Copper(I) complexes with diethylenetriamine (DETA) and *N*,*N*,*N*′,*N*″,*N*″-pentamethyldiethylenetriamine (PMDETA) have been much less extensively studied than the corresponding complexes with bpy-based ligands. Scheme 7 shows the structures of the complexes that have been isolated and characterized so far. In all complexes, DETA and PMDETA act as tridentate ligands. Since, $[Cu^I(PMDETA)]^+$ cations are formally $16e^-$ systems, the fourth coordination site is typically occupied by monodentate ligands such as CO, CH_3CN, or olefin/monomer.

$[Cu^I(DETA)(CO)]^+[BPh_4]^-$ has been prepared in CO saturated methanol by reacting Cu^II with DETA and $NaBPh_4$ [214]. The $[Cu^I(DETA)(CO)]^+$ cation has distorted tetrahedral geometry. The Cu^I center is coordinated by three nitrogen atoms from the DETA ligand (Cu–N(1) = 2.085(4) Å, Cu–N(2) = 2.123(3) Å and Cu–N(3) = 2.073 (4) Å) and one carbon atom of the CO moiety (Cu–C = 1.776(5) Å). The central nitrogen atom in DETA bonds at a significantly longer distance (2.123(3) Å) than do the terminal nitrogens (mean value of 2.079(4) Å). The C–O bond length (1.776(5) Å) and stretching frequency (υ_{CO} = 2080 cm^{-1}) in coordinated CO are similar to other copper(I) complexes with CO ligands [215–217]. The Cu–C≡O angle is nearly linear (176.57(54)°).

The structure of $[Cu^I(DETA)(1\text{-}Hex)]^+[BPh_4]^-$ is similar to that of $[Cu^I(DETA)(CO)]^+[BPh_4]^-$ except that the pseudo tetrahedral coordination around the Cu^I cation is completed by a π-interaction with the double bond of 1-hexene [218]. The deviation from the ideal tetrahedral geometry is

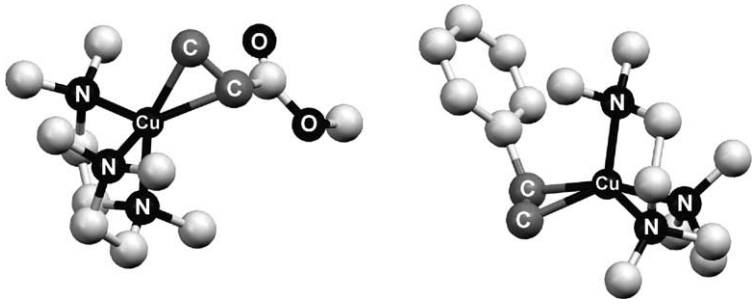

Fig. 7. Molecular structures of $[Cu^{I}(PMDETA)(\pi\text{-styrene})]^{+}$ and $[Cu^{I}(PMDETA)(\pi\text{-methyl acrylate})]^{+}$ cations.

mainly given by L–Cu–L angles (L = N or C) which range from 83.2(7)° to 127.4(9)°. The Cu–N bond lengths in the complex are Cu–N(1) = 2.11(1) Å, Cu–N(2) = 2.25(1) Å and Cu–N(3) = 2.09(1) Å, with the central nitrogen atom being further away from the Cu^{I} center than the terminal nitrogens. The Cu–C bond distances in hexene (2.10(2) and 2.13(2) Å) are in agreement with the distances in other Cu^{I}/1-hexene complexes [219]. The C=C bond distance of the coordinated 1-hexene was observed to be essentially unchanged from that in the free molecule [220]. Furthermore, the C=C–C angle in 1-hexene (120°) is unaffected by coordination to the Cu^{I} center.

$[Cu^{I}(PMDETA)(CH_3CN)]^{+}[ClO_4]^{-}$ complex was prepared by the reaction of $[Cu^{I}(CH_3CN)_4]^{+}[ClO_4]^{-}$ with 1 eq. of PMDETA ligand. $[Cu^{I}(PMDETA)(CO)]^{+}[ClO_4]^{-}$ complex was isolated by treating a methanol solution of $[Cu^{I}(PMDETA)(CH_3CN)]^{+}[ClO_4]^{-}$ with CO [218]. The molecular structures of both complexes could not be obtained by X-ray crystallography due to the unsuitable crystal sizes. However, the stoichiometry and composition was confirmed by elemental analysis. Furthermore, the observation of υ_{CO} bands of the $[Cu^{I}(PMDETA)(CO)]^{+}[BPh_4]^{-}$ at 2082 cm^{-1} (KBr pellet) and 2088 cm^{-1} (aqueous solution) indicate end-on CO coordination as observed in other Cu^{I} complexes with CO [215–217].

We were recently able to isolate and characterize novel $[Cu^{I}(PMDETA)(\pi\text{-M})]^{+}[BPh_4]^{-}$ (M = styrene, methyl acrylate, methyl methacrylate and 1-octene) complexes [221,222]. Molecular structures of $[Cu^{I}(PMDETA)(\pi\text{-styrene})]^{+}$ and $[Cu^{I}(PMDETA)(\pi\text{-methyl acrylate})]^{+}$ cations are shown in Fig. 7. Similarly to DETA, in all complexes PMDETA acts as a tridentate ligand, while the pseudotetrahedral coordination geometry around Cu^{I} is completed by a π-interaction with the C=C double bond of monomer in the presence of a non-coordinating counter-ion (BPh_4^{-}). A slight lengthening of the C=C vinyl double bond upon coordination and a decrease in C=C IR stretching frequencies of $\Delta\upsilon(C{=}C) = -110$, -80, -109, and -127 cm^{-1} for complexes with methyl acrylate, styrene, 1-octene, and methyl methacrylate, respectively, characterize the bonding of the Cu^{I}-olefin complex. Furthermore, the extent of the upfield shift of the vinyl proton resonances upon coordination confirms the presence of significant π-back-bonding.

The results of the EXAFS analysis of $Cu^{I}Br$/PMDETA in methyl acrylate, styrene, toluene and methanol indicated similar structural features of the complex [193]. In all solvents, the EXAFS data were well fit by a structural model that included on average 3.0 nitrogen atoms at the distance of 2.12 Å and 1.0 bromine atom at the distance of 2.33 Å. The average Cu^{I}–N bond length was in agreement with other Cu^{I} complexes with similar nitrogen based chromophores [223]. On the other hand, Cu^{I}–Br bond distance indicated covalent bonding to the Cu^{I} center. Based on these results, one structure that is consistent with the EXAFS analysis includes neutral $[Cu^{I}(PMDETA)Br]$ complex. However, other structures might also coexist in an equilibrium and are shown in Scheme 8. Based on the solvent polarity and temperature, the dissociation of bromide anions can lead to the formation of an ionic $[Cu^{I}(PMDETA)]^{+}[Br]^{-}$ complex. The coordinatively unsaturated $[Cu^{I}(PMDETA)]^{+}$ cation can be further coordinated by solvent or monomer leading to the formation of $[Cu^{I}(PMDETA)(S)]^{+}[Br]^{-}$ and $[Cu^{I}(PMDETA)(M)]^{+}[Br]^{-}$, respectively, as demonstrated in the case of $[BPh_4]^{-}$ analogues.

3.2.2. *tpy and tpy derivatives*

Substituted terpyridine, 4,4′,4″-tris(5-nonyl)-2,2′:6′,2″-terpyridine (tNtpy), is a planar tridentate ligand that was suc-

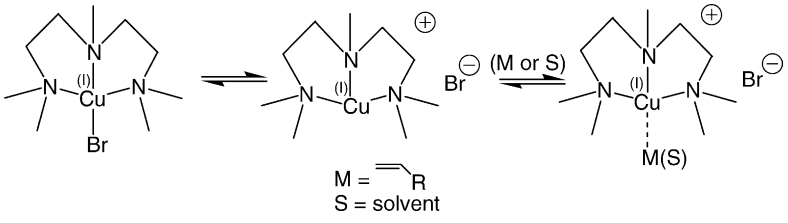

Scheme 8. Proposed structures for $Cu^{I}Br$/PMDETA complex.

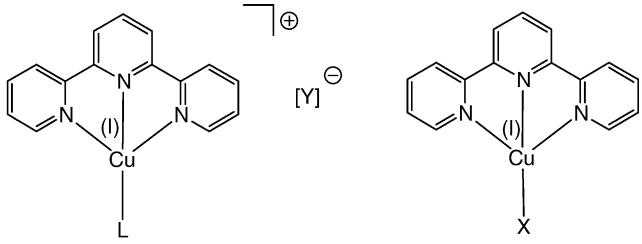

L = CH_3CN, CO, olefin, etc.
X = halide
Y = noncoordinating anion

Scheme 9. General structures of Cu^I complexes with tpy based ligands.

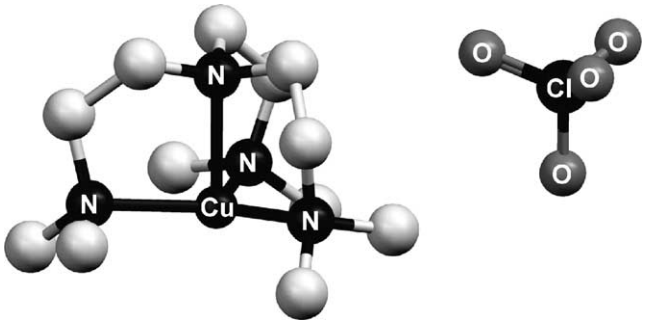

Fig. 8. Molecular structure of $[Cu^I(Me_6TREN)]^+[ClO_4]^-$ [229].

cessfully used in the homogeneous ATRP of methyl acrylate and styrene. The polymerization of both monomers was controlled and the resulting polymers had relatively low polydispersities ($M_w/M_n < 1.2$) [142]. Similar to PMDETA, the typical ligand to copper(I) halide ratio used in the polymerization was 1:1.

Copper(I) complexes with 2,2′:6,2″-terpyridine (tpy) based ligands should have a coordination sphere similar to that of copper(I) complexes with DETA and PMDETA ligands discussed above. Therefore, tpy and derivatives are expected to form tetra-coordinated complexes with copper(I) in which the fourth coordination sphere is occupied by a monodentate ligand (Scheme 9). This has been demonstrated in the isolation and elemental analysis of $[Cu^I(tpy)Br]$ [224], $[Cu^I(tpy)(py)]^+[ClO_4]^-$ (py = pyridine) [225,226], and $[Cu^I(tpy)(CH_3CN)]^+[CH_3COO]^-$ [227] complexes.

The EXAFS-determined structural data of Cu^IBr complex with tNtpy ligand in methyl acrylate indicated that the coordination sphere around Cu^I center is occupied by on average 2.7 nitrogen atoms at the distance of 2.03 Å and 1.0 bromine atoms at the distance of 2.29 Å [193]. The coordination numbers and distances in styrene indicate similar structural features of the complex. The EXAFS data in methyl acrylate and styrene were consistent with a neutral $[Cu^I(tNtpy)Br]$ complex. However, as discussed earlier in the case of Cu^IBr complex with tridentate PMDETA, other species might coexist in an equilibrium such as $[Cu^I(tNtpy)(S)]^+[Br]^-$ (S = solvent or monomer).

3.3. Tetradentate ligands

1,1,4,7,10,10-Hexamethyltriethylenetetramine (HMTETA) is a tetradentate amine ligand that was successfully used in the ATRP of styrene, methyl acrylate and methyl methacrylate [144]. The ligand to Cu^IBr ratio used in the polymerization was 1:1. Also, on the other hand, Cu^IBr complex with tris[2-(dimethylamino)ethyl]amine (Me_6TREN) showed a very high activity for methyl acrylate polymerization, enabling fast and controlled polymerization at ambient temperature [145]. Furthermore, 1,4,8,11-tetraaza-1, 4, 8, 11-tetramethylcyclotetradecane ($Me_4CYCLAM$) is the only tetradentate cyclic amine that was investigated in the ATRP. In conjunction with Cu^IBr or Cu^ICl, this catalytic system does not enable good control over ATRP of various monomers. The principal reason is very slow deactivation rate constant (k_d) which increases radical concentration and consequently radical termination rates [228].

Structures of copper(I) complexes with tetradentate nitrogen based ligands TREN, Me_6TREN, TETA, HMTETA, CYCLAM and $Me_4CYCLAM$ are very rare. The principal problem in isolating the corresponding copper(I) complexes is the fact that they are extremely air and moisture sensitive. Schindler and coworkers have succeeded in isolating crystals of $[Cu^I(Me_6TREN)]^+[ClO_4]^-$ complex [229]. The X-ray structure of the complex (Fig. 8) indicated that copper(I) cation is coordinated by four nitrogen atoms of Me_6TREN ligand (Cu^I–N (equatorial) = 2.122(7) Å and Cu^I–N (axial) = 2.200(14) Å). The copper(I) center in $[Cu^I(Me_6TREN)]^+[ClO_4]^-$ can be formally described as trigonal pyramidal due to the weak interaction with the perchlorate anion (Cu^I–O = 3.53(1) Å).

The X-ray structure of $[Cu^I(HMTETA)]^+[Cu^ICl_2]^-$ complex (Fig. 9) which was synthesized by the reaction of Cu^ICl with 1 eq. of HMTETA ligand in CH_3CN indicated that in the case of HMTETA ligand, the copper(I) center is distorted tetrahedral in geometry (Cu^I–N = 2.009(5), 2.015(5), 2.202(6) and 2.218(6) Å) [230]. $[Cu^ICl_2]^-$ anions in the complex are linear with Cu^I–Cl distances of 2.107(4) and 2.086(2) Å.

Based on these results, one should generally expect that copper(I) complexes with tetradentate nitrogen based ligands should be ionic with the general formula $[Cu^IN_4]^+[Y]^-$. The counter-ions, Y^-, are usually non- or partially coordinating such as ClO_4^-, but they can also be linear $[Cu^IX_2]^-$ (X = halide) as observed in $[Cu^I(HMTETA)]^+[Cu^ICl_2]^-$. With regard to halide anions, there have been additional reports in the literature which suggested that the copper(I) halide complexes with tetradentate nitrogen based ligands could have a general structure $[Cu^IN_4'X]$, where N_4' denotes a tricoordinated ligand [231–234]. In such cases, the copper complexes are neutral with the copper(I) center being coordinated by three nitrogen atoms of a tetradentate ligand and one halogen atom.

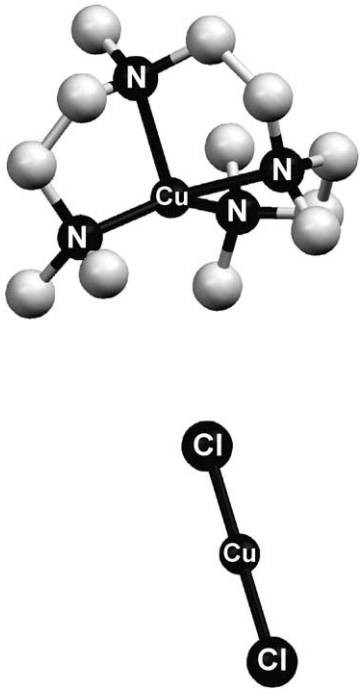

Fig. 9. Molecular structure of $[Cu^{I}(HMTETA)]^{+}[Cu^{I}Cl_2]^{-}$ [230].

The results of EXAFS measurements of $Cu^{I}Br$ complex with Me_6TREN ligand in different solvents are summarized in Table 5 [193]. The Cu K-edge EXAFS spectrum in styrene was best modeled assuming that the coordination sphere around Cu^{I} is occupied by on average 3.0 nitrogen atoms at the distance of 2.15 Å and 1.2 bromine atoms at the distance of 2.33 Å. The results in methyl acrylate and toluene were analogous, indicating similar structural features of the complex. Taking into account the $18e^{-}$ rule and tetradentate nature of Me_6TREN ligand, one would expect that the most probable structure of $Cu^{I}Br/Me_6TREN$ complex in solution would be $[Cu^{I}(Me_6TREN)]^{+}[Br]^{-}$. The average Cu^{I}–N bond length in styrene (2.15 Å), methyl acrylate (2.15 Å) and toluene (2.14 Å) is in agreement with a previously characterized $[Cu^{I}(Me_6TREN)]^{+}[ClO_4]^{-}$ complex (2.161 Å) [230]. However, the coordination number of nitrogen appears to be rather low for a tetradentate Me_6TREN ligand. Additionally, the presence of Br backscatterer in the spectrum of the Cu K-edge indicated covalent bonding to the Cu^{I} center. This evidence contradicts the presence of solely ionic $[Cu^{I}(Me_6TREN)]^{+}[Br]^{-}$ species. The presence of Cu^{I}–Br absorbance in the EXAFS spectra of $Cu^{I}Br/Me_6TREN$ could suggest the presence of linear $[Cu^{I}Br_2]^{-}$ anions, as described earlier in the case of $[Cu^{I}(dNbpy)_2]^{+}[Cu^{I}Br_2]^{-}$ complex. However, the average Cu^{I}–Br bond distance in styrene (2.33 Å), methyl acrylate (2.33 Å) and toluene (2.31 Å) appears to be longer than the Cu^{I}–Br bond distance in Cu^{I} complexes with $[Cu^{I}Br_2]^{-}$ anions (2.206–2.232 Å) [155,159,160,235]. The elongation of Cu^{I}–Br bond in $[Cu^{I}Br_2]^{-}$ anions is possible, but was not observed in structurally related $[Cu^{I}(HMTETA)]^{+}[Cu^{I}Cl_2]^{-}$ (HMTETA = 1,1,4,7,10,10-hexamethyltriethylenetetramine) complex, in which the Cu^{I}–Cl bond length was found to be similar to other Cu^{I} complexes with linear $[Cu^{I}Cl_2]^{-}$ anions [230].

The structure of the $Cu^{I}Br/Me_6TREN$ complex that is consistent with the EXAFS analysis points to the presence of a neutral $[Cu^{I}(Me_6TREN')Br]$ complex (Me_6TREN' denotes a tricoordinated Me_6TREN). Similar structures were proposed earlier in copper [231] and cobalt [232] complexes with Me_6TREN ligand in order to explain the kinetics of ligand substitution reactions. Furthermore, the dechelation of one "amine" arm in Cu^{II} complexes with other tetradentate nitrogen based ligands has also been reported [233,234]. Due to the sensitivity of EXAFS measurements and also the possibility for the coexistence of more than one species in an equilibrium, all complexes discussed above can be present in solution. The proposed structures are shown in Scheme 10.

The Cu K-edge EXAFS spectrum of $Cu^{I}Br/Me_4CYCLAM$ complex in methyl acrylate was well fit assuming the structural model that included on average 3.8 nitrogen atoms at the distance of 2.06 Å and 1.7 bromine atoms at the distance of 2.23 Å [193]. In more polar medium

Table 5
Structural parameters of $Cu^{I}Br$ complex with Me_6TREN ligand, determined by EXAFS measurements under ambient conditions at the Cu K- and Br K-edge

Solvent	Backscattering	N	r (Å)	σ (Å)	ΔE_0 (eV)	k (Å^{-1})	Fit index
Styrene	Cu—N	3.0	2.15	0.114	14.8	4.2–15.6	15.4
	Cu—Br	1.2	2.33	0.080			
	Cu—C	4.0	2.95	0.105			
	Br—Cu	1.0	2.32	0.071	19.1	3.6–14.0	17.1
MA	Cu—N	2.8	2.15	0.110	15.3	4.2–15.4	12.3
	Cu—Br	1.1	2.33	0.077			
	Cu—C	5.9	2.94	0.116			
	Br—Cu	1.0	2.32	0.077	18.6	4.2–13.1	14.6
Toluene	Cu—N	2.8	2.14	0.100	18.6	4.2–14.6	20.8
	Cu—Br	1.3	2.31	0.084			
	Cu—C	5.4	2.91	0.118			
	Br—Cu	1.2	2.31	0.086	21.8	3.8–14.0	18.0

N: coordination number, r: absorber–backscatterer distance, σ: Debye–Waller factor. Inherent errors are 10–15% for coordination numbers and Debye–Waller factors and 1% for distances.

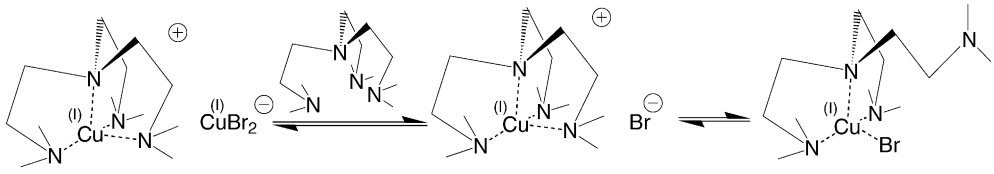

Scheme 10. Proposed structures for $Cu^{I}Br/Me_6TREN$ complex.

(MA/MeOH = 3:1 vol.), the signal due to the coordinated bromine atoms disappeared and only nitrogen backscatterers are visible in the FT Cu K-edge EXAFS spectrum. The average Cu^{I}–N bond length for $Cu^{I}Br/Me_4CYCLAM$ complex in methyl acrylate (2.06 Å) and methyl acrylate/MeOH (3:1 vol.) (2.05 Å) was shorter than the average Cu^{I}–N bond lengths in related $[Cu^{I}(HMTETA)]^{+}[Cu^{I}Cl_2]^{-}$ (Cu^{I}–N_{AV} = 2.111 Å) [230] and $[Cu^{I}(Me_6TREN)]^{+}[ClO_4]^{-}$ complexes (Cu^{I}–N_{AV} = 2.161 Å) [229]. The shortening of the average Cu^{I}–N bond length in $Cu^{I}Br/Me_4CYCLAM$ could be due to the steric strain imposed by cyclic $Me_4CYCLAM$ ligand as described in the literature [236,237]. Copper(I) complexes with $Me_4CYCLAM$ ligand are therefore expected to adopt square planar geometry as opposed to tetrahedral and square pyramidal structures observed in $[Cu^{I}(HMTETA)]^{+}[Cu^{I}Cl_2]^{-}$ and $[Cu^{I}(Me_6TREN)]^{+}[ClO_4]^{-}$, respectively. The average Cu^{I}–Br bond length and coordination number of bromine in $Cu^{I}Br/Me_4CYCLAM$ complex in methyl acrylate are consistent with Cu^{I} complexes with $[Cu^{I}Br_2]^{-}$ anions (2.206–2.232 Å) [155,159,160,235]. Similar to $Cu^{I}Br/Me_6TREN$ discussed earlier, the EXAFS results of $Cu^{I}Br/Me_4CYCLAM$ complex in methyl acrylate are consistent with $[Cu^{I}(Me_4CYCLAM)]^{+}[Cu^{I}Br_2]^{-}$. In more polar medium, the complex predominantly exists as $[Cu^{I}(Me_4CYCLAM)]^{+}[Br]^{-}$. The 1:1/2 stoichiometry in $[Cu^{I}(Me_4CYCLAM)]^{+}[Cu^{I}Br_2]^{-}$ indicates the presence of free $Me_4CYCLAM$ ligand in the ATRP system since the catalyst is typically prepared by mixing $Cu^{I}Br$ with equimolar amount of $Me_4CYCLAM$. Consequently, the free ligand can participate in chain transfer reactions which limit the control of the polymerization at higher molecular weights, as observed previously in the case of PMDETA ligand [238,239].

4. Copper(II) complexes with nitrogen based ligands

4.1. Bidentate ligands

4.1.1. bpy and bpy derivatives

4.1.1.1. Solid state studies. Copper(II) complexes with bpy based ligands are typically synthesized by reacting the corresponding $Cu^{II}Y_2$ salts (Y = PF_6^{-}, $CF_3SO_3^{-}$, ClO_4^{-}, etc.) or $Cu^{II}X_2$ salts (X = Cl^{-}, Br^{-} and I^{-}) with 2 eq. of bpy ligand. In the case of non-coordinating anions Y, the corresponding isolated complexes have the general formula $[Cu^{II}(bpy)_2]^{2+}[Y]_2^{-}$ and $[Cu^{II}(bpy)_3]^{2+}[Y]_2^{-}$. In the case of halides, $[Cu^{II}(bpy)_2X]^{+}[X]^{-}$ are typically formed. Additionally, halide anions in $[Cu^{II}(bpy)_2X]^{+}[X]^{-}$ can be replaced by Y^{-} anions, yielding $[Cu^{II}(bpy)_2X]^{+}[Y]^{-}$ complexes.

$[Cu^{II}(bpy)_2]^{2+}[Y]_2^{-}$ complexes are rare, and up to date only one such complex, distorted tetrahedral $[Cu^{II}(bpy)_2]^{2+}[PF_6]_2^{-}$ has been isolated and characterized in the solid state [151]. The principle reason is the strong tendency of Cu^{II} complexes to adopt penta- and hexacoordinated geometries. Earlier attempts to isolate $[Cu^{II}(bpy)_2]^{2+}$ cations were unsuccessful yielding Cu^{II} complexes that were either pentacoordinated as observed in $[Cu^{II}(bpy)_2(H_2O)]^{2+}[PF_6]_2^{-}$ [240,241], or hexacoordinated in $[Cu^{II}(bpy)_2(F_2BF_2)]^{+}[BF_4]^{-}$ [242] and $[Cu^{II}(bpy)_2(O_2ClO_2)]^{+}[ClO_4]^{-}$ [242,243].

Copper(II) cations with three coordinated bpy ligands have also been reported. They are usually synthesized as described above with the exception that three or more equivalents of bpy ligands are added to Cu^{II} salts. $[Cu^{II}(bpy)_3]^{2+}$ are typically octahedral in geometry as observed in $[Cu^{II}(bpy)_3]^{2+}[ClO_4]_2^{-}$ complex [244].

As evident from the number of X-ray data available, by far the most common Cu^{II} complexes with bpy ligands involve $[Cu^{II}(bpy)_2X]^{+}[X]^{-}$ and $[Cu^{II}(bpy)_2X]^{+}[Y]^{-}$. Complexes with $[Cu^{II}(bpy)_2X]^{+}$ cations (Fig. 10) [245] are particularly important in the ATRP as they are responsible for the deactivation process. Structural data for a series of $[Cu^{II}(bpy)_2Cl]^{+}[Y]^{-}$ complexes are shown in Table 6 [246–251]. The corresponding data for $[Cu^{II}(bpy)_2Br]^{+}[Y]^{-}$ and $[Cu^{II}(bpy)_2I]^{+}[Y]^{-}$ complexes are summarized in Table 7 [245,251–254] and Table 8 [251,252,255], respectively. The τ parameter is calculated as: $\tau = (\varphi_1 - \varphi_2)/60$, where φ_1 and φ_2 are the largest and second largest N–Cu^{II}–N angles [248,256]. The value of $\tau = 1$ corresponds to regular trigonal bipyramidal (RTBP) and $\tau = 0$ to regular square pyramidal geometry (RSP). The two geometries are shown in Scheme 11.

For $[Cu^{II}(bpy)_2Cl]^{+}[Y]^{-}$ complexes (Table 6), the structure of the pentacoordinated CuN_4Cl chromophore varies from near RTBP to intermediate between RTBP and RSP. This is reflected in a range of τ values from 1.00 to 0.53. The bond lengths and τ values for $[Cu^{II}(bpy)_2Br]^{+}[Y]^{-}$ complexes are shown in Table 7, the table shows a comparable range of τ values. $[Cu^{II}(dNbpy)_2Br]^{+}[Cu^{I}Br_2]^{-}$, which has been isolated from the ATRP of styrene, shows perfect RTBP geometry (Fig. 11) [254]. This could be due to the presence of linear $[Cu^{I}Br_2]^{-}$ anions, or long alkyl chains in the 4,4′-positions of the bpy ligands. It was generally observed that substituted bpy derivatives $[Cu^{II}(bpy)_2Br]^{+}$ usu-

Table 6
Structural data for $[Cu^{II}(bpy)_2Cl]^+[Y]^-$ complexes

Y	$[PF_6]^-\cdot H_2O$ [246]	$[Cl]^-\cdot 6H_2O$ [247]	$[NO_3]^-\cdot 3H_2O$ [248]	$[Cu^ICl_2]^-$ [249]	$[BF_4]^-$ [250]	$[CF_3SO_3]^-$ [251]	$[ClO_4]^-$ [248]	$[CF_3(CF_2)_3SO_3]^-$ [251]	$[CF_3SO_3]^-\cdot H_2O$ [251]
Cu^{II}—Cl	2.344(2)	2.361(4)	2.308(3)	2.356	2.285(3)	2.259(1)	2.263(3)	2.284(2)	2.246(2)
Cu^{II}—N(1)	1.996(6)	1.989(10)	1.989(6)	1.985	2.006(7)	1.986(5)	1.993(4)	1.993(6)	1.981(4)
Cu^{II}—N(2)	2.105(6)	2.077(10)	2.089(6)	2.063	2.079(8)	2.091(4)	2.076(3)	2.061(6)	2.083(4)
Cu^{II}—N(3)	2.005(6)	1.970(10)	1.989(6)	1.995	1.983(7)	1.973(4)	1.991(4)	1.969(6)	1.995(4)
Cu^{II}—N(4)	2.108(6)	2.087(10)	2.112(5)	2.086	2.142(8)	2.128(3)	2.136(5)	2.140(6)	2.140(4)
τ	1.00	0.99	0.79	0.70	0.67	0.67	0.62	0.62	0.53

Table 7
Structural data for $[Cu^{II}(bpy)_2Br]^+[Y]^-$ complexes

Y	$[PF_6]^-\cdot H_2O$ [251]	$[NO_3]^-\cdot H_2O$ [251]	$[ClO_4]^-$ [251]	$[Br]^-$ [245]	$[BF_4]^-$ [252]	$[BPh_4]^-$ [251]	$[CF_3SO_3]^-$ [251]	$[CF_3SO_3]^-\cdot CH_3CN$ [253]	$[Cu^IBr_2]^-$[a] [254]
Cu^{II}—Br	2.469(1)	2.514(1)	2.466(1)	2.429(2)	2.419(3)	2.419(1)	2.418(1)	2.418(3)	2.426(3)
Cu^{II}—N(1)	1.991(3)	1.982(4)	1.986(3)	1.977(6)	1.996(7)	1.984(2)	1.997(4)	1.986(2)	1.946(13)
Cu^{II}—N(2)	2.093(3)	2.082(4)	2.094(3)	2.075(8)	2.068(8)	2.105(3)	2.067(4)	2.086(2)	1.977(15)
Cu^{II}—N(3)	1.990(3)	1.991(4)	1.999(3)	1.978(6)	1.995(7)	1.981(2)	2.002(4)	2.003(4)	2.051(15)
Cu^{II}—N(4)	2.096(3)	2.089(4)	2.098(3)	2.085(7)	2.114(9)	2.131(3)	2.169(5)	2.163(4)	2.088(16)
τ	0.91	0.89	0.85	0.81	0.69	0.58	0.49	0.49	1.00

[a] Crystal structure of $[Cu^{II}(dNbpy)_2Br]^+[Cu^IBr_2]^-$.

ally have τ values between 0.85 and 1.00, indicating that their geometry is closer to the RTBP limit [153]. As indicated in Table 8, $[Cu^{II}(bpy)_2I]^+[Y]^-$ complexes show a much more limited range of distortion from the RTBP stereochemistry, $\tau = 0.90–0.85$. Cu^{II}–X bond lengths in $[Cu^{II}(bpy)_2X]^+[Y]^-$ complexes are affected by τ values, and generally decrease as τ decreases.

Similar structural studies have also been conducted previously on $[Cu^{II}(phen)_2X]^+[Y]^-$ complexes [257,258]. Close similarity between the phen/X and bpy/X complexes was observed.

With respect to $Cu^{II}Br_2$ complexes with bpy based ligands, an additional mode of coordination was observed which involved the formation of a 1:1 adduct between $Cu^{II}Br_2$ and bpy ligand. This was demonstrated in the isolation and characterization of neutral $[Cu^{II}(bpy)Br_2]$ [259] and $[Cu^{II}(dNbpy)Br_2]$ [253] complexes. In $[Cu^{II}(bpy)Br_2]$, each Cu^{II} site is coordinated by two nitrogen atoms of a single bipyridine ligand (Cu^{II}–N = 2.022(3) Å), and two bromine atoms (Cu^{II}–Br = 2.4224(7) Å). The square planar motifs are stacked stepwise to form one-dimensional chains via long, semicoordinate Cu^{II}–Br bonds (Cu^{II}–Br = 3.1371(1) Å), as shown in Fig. 12. This results in a distorted 4 + 2 octahedral coordination geometry, which is typically observed in Cu^{II}/halide complexes with $Cu^{II}N_2X_2$ chromophore (X = Br or Cl) [260].

Fig. 13 shows the molecular structure of structurally related $[Cu^{II}(dNbpy)Br_2]$ complex which was synthesized by stoichiometric reaction between $Cu^{II}Br_2$ and dNbpy. The Cu–N and Cu–Br bond lengths in $[Cu^{II}(dNbpy)Br_2]$ (Cu–N = 2.011(7), 2.022(7) Å, Cu–Br = 2.3621(14), 2.3567(13) Å) are slightly shorter when compared with the $Cu^{II}(bpy)Br_2$ analogue (Cu–N = 2.033(3) Å, Cu–Br = 2.4224(7) Å). In $[Cu^{II}(dNbpy)Br_2]$, however, the shortest distance between the Cu atom and the Br atom which does not belong to the same molecule is approximately 5.8 Å, which rules out the possibility of formation of semicoordinate bonds observed in $Cu^{II}(bpy)Br_2$ analogue. One reason for this is the steric hindrance imposed on the complex by the long alkyl chains of the dNbpy ligand which are aligned perpendicularly to the bipyridine planes. This structural modification of the bpy ligand could also be responsible for the unusual 1:1 complex between $Cu^{II}Br_2$ and dNbpy due to a weakening of the binding constant of dNbpy to $Cu^{II}Br_2$, as will be discussed in the next section.

Table 8
Structural data for $[Cu^{II}(bpy)_2I]^+[Y]^-$ complexes

Y	$[I]^-$ [255]	$[PF_6]^-$ [251]	$[ClO_4]^-$ [252]	$[BPh_4]^-$ [251]	$[CF_3SO_3]^-$ [251]
Cu^{II}—I	2.70(4)	2.688(1)	2.675(4)	2.676(1)	2.676(1)
Cu^{II}—N(1)	2.00(4)	1.993(4)	1.989(6)	1.989(3)	1.990(5)
Cu^{II}—N(2)	1.96(4)	2.084(4)	2.090(8)	2.103(3)	2.096(5)
Cu^{II}—N(3)	2.03(4)	1.990(4)	1.987(6)	2.000(3)	1.989(5)
Cu^{II}—N(4)	2.10(4)	2.090(4)	2.100(7)	2.103(3)	2.107(6)
τ	0.90	0.89	0.86	0.80	0.85

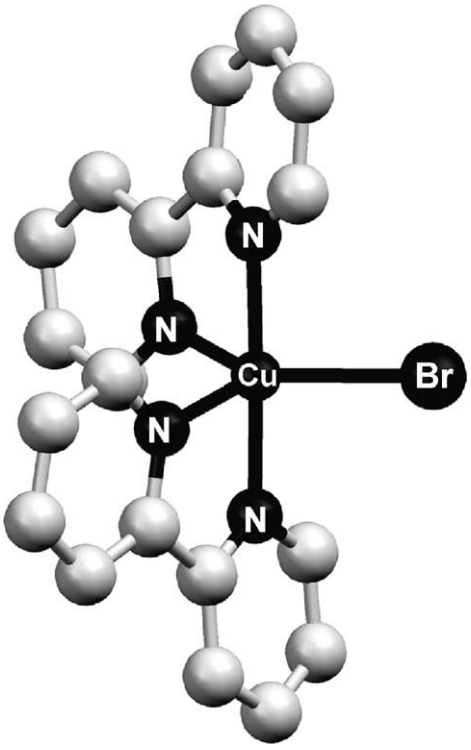

Fig. 10. Structure of $[Cu^{II}(bpy)_2Br]^+$ cation in $[Cu^{II}(bpy)_2Br]^+[Br]^-$ [245].

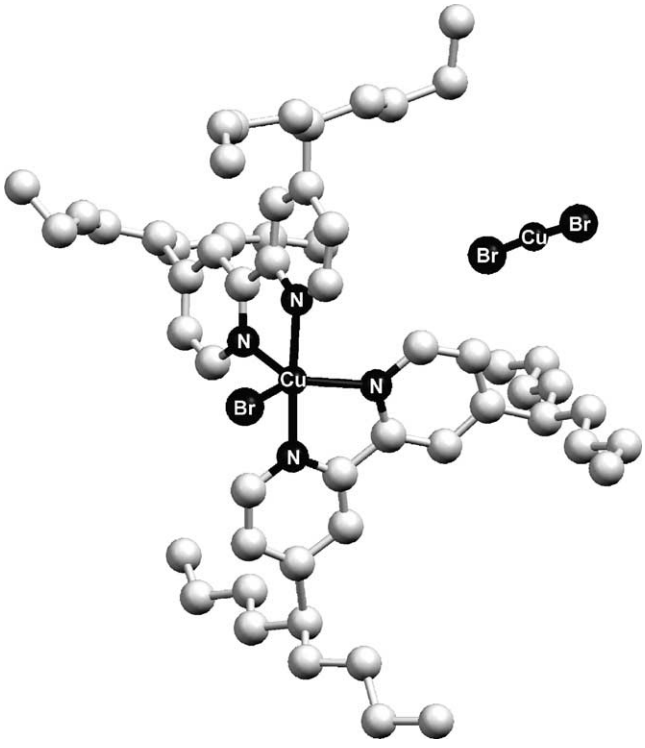

Fig. 11. Molecular structure of $[Cu^{II}(dNbpy)_2Br]^+[Cu^{I}Br_2]^-$.

The structures of $Cu^{II}X_2$ complexes with bidentate AlkPMI ligands, which are also commonly used in copper mediated ATRP, have not been as widely studied. However, they are expected to show similar structural features to bpy and its derivatives.

4.1.1.2. Solution studies. Calorimetry and UV–vis spectroscopy: Complexation of Cu^{II} cations with nitrogen-containing bidentate ligands such as 1,10-phenenthroline and 2,2′-bipyridine has been extensively studied using calorimetry and spectrophotometric techniques in a number of solvents [261–266]. The technique for data analysis typically employs stepwise equilibrium coordination as illustrated in Scheme 12, where Mt corresponds to the metal and N the maximum number of ligands L the metal can coordinate [267]. If one defines stepwise equilibrium constants $\beta_0 = 1$, $\beta_1 = K_1$, $\beta_2 = K_1K_2$, $\beta_n = K_1K_2$, …, K_N, then the total metal concentration in solution can be expressed as:

$$T_{Mt} = [Mt] + [MtL] + [MtL_2] + \cdots + [MtL_N],$$

$$[Mt] = \beta_0[Mt][L],$$

$$[MtL] = \beta_1[Mt][L], \quad [MtL_2] = \beta_2[Mt][L]^2,$$

$$T_{Mt} = [Mt]\sum_{n=0}^{N} \beta_n[L]^n \tag{1}$$

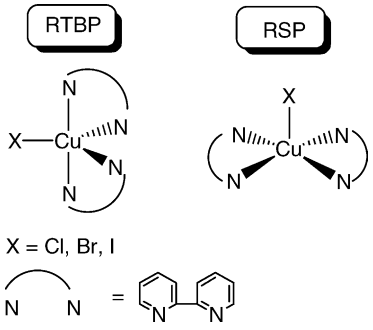

Scheme 11. Regular trigonal bipyramidal (RTBP) and square pyramidal (RSP) geometries for $[Cu^{II}(bpy)_2X]^+$ cation.

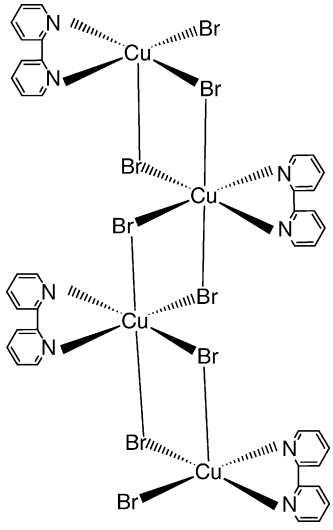

Fig. 12. Schematic representation of one-dimensional chain structure of $[Cu^{II}(bpy)Br_2]$, showing the long semicoordinate Cu^{II}—Br bonds.

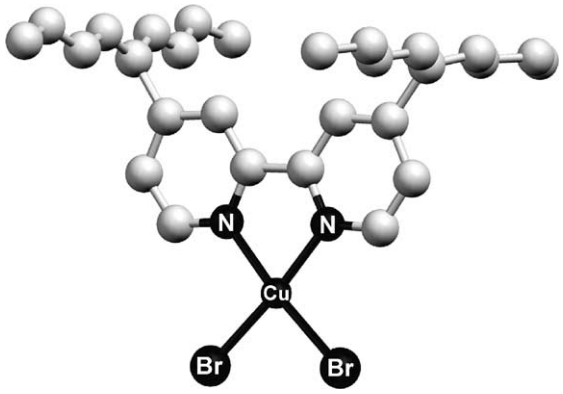

Fig. 13. Molecular structure of $[Cu^{II}(dNbpy)Br_2]$.

Similarly, the total ligand concentration in solution is given by

$$T_L = [L] + [MtL] + 2[MtL_2] + \cdots + N[MtL_N],$$

$$T_L = [L] + [Mt]\sum_{n=0}^{N} n\beta_n[L]^n \quad (2)$$

In order to calculate the relative percentages of each species present in solution, the concept of average ligand number is typically introduced. It is the ratio of total ligand concentration bound to the metal to the total metal concentration itself:

$$\bar{n} = \frac{T_L - [L]}{T_{Mt}} = \frac{[MtL] + 2[MtL_2] + 3[MtL_3] + \cdots + N[MtL_N]}{[Mt] + [MtL] + [MtL_2] + \cdots + [MtL_N]},$$

$$\bar{n} = \frac{\sum_{n=0}^{N} n\beta_n[L]^n}{\sum_{n=0}^{N} \beta_n[L]^n} \quad (3)$$

Having defined the average ligand number, the degree of formation of the individual components in the mixture (or their mole fraction) is given by

$$\alpha = \frac{\bar{n}}{N}, \qquad \alpha_{MtL_j} = \alpha_j = \frac{\beta_j[L]^j}{\sum_{n=0}^{N} \beta_n[L]^n} \quad (4)$$

$$Mt + L \rightleftharpoons MtL \qquad K_1 = \frac{[MtL]}{[Mt][L]}$$

$$MtL + L \rightleftharpoons MtL_2 \qquad K_2 = \frac{[MtL_2]}{[MtL][L]}$$

$$\vdots \qquad\qquad \vdots$$

$$MtL_{N-1} + L \rightleftharpoons MtL_N \qquad K_N = \frac{[MtL_N]}{[MtL_{N-1}][L]}$$

Scheme 12. Stepwise equilibrium for the coordination of the ligand to the metal ion.

Knowing the individual formation constants for each species present in solution, one can with the above formula construct a plot that relates the equilibrium concentration of the ligand to the fraction of the species. However, usually, the equilibrium concentration of the ligand is not known, and the information about the total ligand concentration is readily available. Ratio of the total metal to ligand concentration in the system can be related to the individual formation constants by the following relationship:

$$q = \frac{T_L}{T_{Mt}} = \frac{[L]}{T_{Mt}} + \bar{n}, \quad T_{Mt} = \frac{\sum_{n=0}^{N} \beta_n[L]^{n+1}}{\sum_{n=0}^{N} (q-n)\beta_n[L]^n} \quad (5)$$

A second plot can now be constructed, which relates the total metal concentration (which is known) to the equilibrium concentration of the ligand for a fixed metal to ligand ratio q. This enables the immediate determination of the relative proportion α of each species present in solution. In the case of $Cu^{II}(OTf)_2$/bpy system, three complexes can form, $[Cu^{II}(bpy)]^{2+}$, $[Cu^{II}(bpy)_2]^{2+}$ and $[Cu^{II}(bpy)_2]^{3+}$. The formation constants for each complex were determined in H_2O previously using calorimetry and the values are shown in Scheme 13 [265]. Using the above methodology, one can construct the formation curves for each complex formed and also relate the equilibrium concentration of bpy ligand to the total Cu^{2+} concentration for a fixed Cu^{2+} to bpy ratios (Eqs. (4) and (5)). The corresponding plots are shown in Fig. 14a and b. From the graphs it can be seen that at a total Cu^{2+} concentration of 1.0×10^{-3} M addition of 0.5 eq. of bpy ligand (5.0×10^{-4} M) will result in the formation of only monocoordinated complex $[Cu(bpy)]^+$. With this ratio, the complexation is incomplete and the reaction medium consists of approximately 50% Cu^{2+} and 50% $[Cu(bpy)]^{2+}$. Using the same total concentration of Cu^{2+} but increasing the number of equivalents of bpy ligand to 2 will result in a formation of $[Cu(bpy)]^{2+}$ (20%), $[Cu(bpy)_2]^{2+}$ (45%) and $[Cu(bpy)_3]^{2+}$ (35%). Therefore, under these conditions, the formation of $[Cu(bpy)_2]^{2+}$ complex is slightly favored. Furthermore, when the number of equivalents of bpy ligand is increased to 4, the majority of Cu^{2+} exists as $[Cu(bpy)_3]^{2+}$ (90%), the remaining 10% being $[Cu(bpy)_2]^{2+}$. From Fig. 14b, it is also interesting to notice that there are ranges of Cu^{2+} concentrations (for a given ligand ratio), where the distribution of species remains constant. Also, on the other hand, the mole fraction of $[Cu(bpy)_2]^{2+}$ under any conditions never exceeds 0.45.

Apart from aqueous medium, the complexation between Cu^{2+} and bpy has also been investigated in DMF [261]. The equilibrium constants according to Scheme 13 were deter-

$$Cu^{2+} + bpy \xrightleftharpoons{\log K_1 = 7.81} [Cu(bpy)]^{2+}$$

$$[Cu(bpy)]^{2+} + bpy \xrightleftharpoons{\log K_2 = 4.64} [Cu(bpy)_2]^{2+}$$

$$[Cu(bpy)_2]^{2+} + bpy \xrightleftharpoons{\log K_3 = 4.17} [Cu(bpy)_3]^{2+}$$

Scheme 13. Equilibrium constants for the formation of $[Cu^{II}(bpy)_n]^{2+}$ complexes in H_2O.

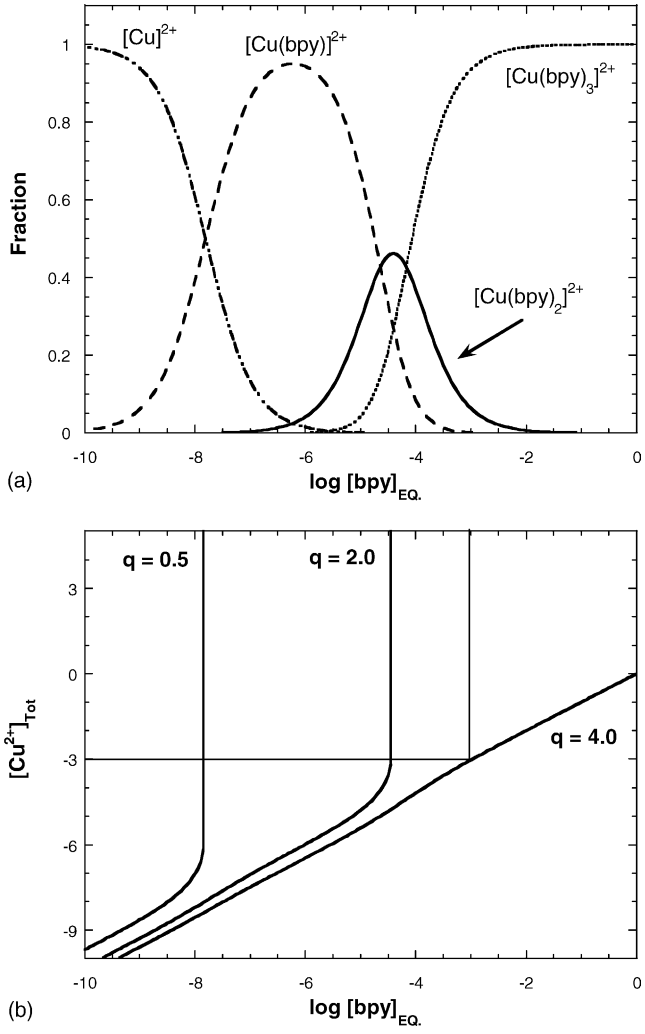

Fig. 14. Extended concentration distribution diagram for Cu^{2+}/bpy equilibrium system in H_2O: (a) formation curve and concentration distribution of complexes; (b) $\log[Cu^{2+}]_{Tot} = f(\log[bpy]_{EQ})$.

mined to be $\log K_1 = 7.20$, $\log K_2 = 3.54$ and $\log K_3 = 1.82$. The equilibrium constant for the formation of $[Cu(bpy)_3]^{2+}$ is lower than the value reported in H_2O. Consequently, $[Cu(bpy)_3]^{2+}$ species in DMF will be formed only at higher concentrations of bpy ligand (Fig. 15). As a result, the maximum molar fraction of $[Cu(bpy)_2]^{2+}$ complex that can be formed will increase.

In the presence of an additional coordinating anion, the analysis of the complexation equilibrium between Cu^{2+} and bpy becomes rather complex. Since we are dealing with a ternary system, a variety of complexes can be formed. One such study focused on the complex equilibrium between Cu^{2+}, bpy and Br^- in DMF [261]. The equilibrium reactions that were taken into account in the data analysis are shown in Scheme 14. Apart from the Cu^{2+} complexes with bpy, mixed complexes between Cu^{2+}, bpy and Br^-, the authors also took into account the complexation between Cu^{2+} and Br^- anions only. The formation of higher order halocuprates in solution with the general formula

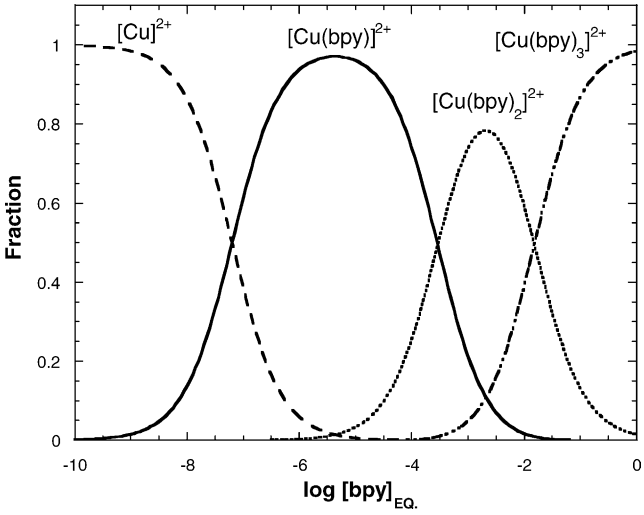

Fig. 15. Formation curves and concentration distribution of $[Cu(bpy)_n]^{2+}$ complexes in DMF.

$[CuX_n]^{2-n}$ (X = Cl or Br) has been subject of numerous investigations [268–273]. From the titration curves obtained, it was indicated that in solutions that contain Cu^{2+}, bpy and Br^- in the molar ratios 1:2:1, respectively, the predominant complex formed was $[Cu^{II}(bpy)_2Br]^+[Br]^-$ (95%). The structure of the $[Cu^{II}(bpy)_2Br]^+$ cation in the complex was also confirmed by UV–vis spectroscopy. Typically CuN_4X^+ chromophores, which have trigonal bipyramidal geometry, show a maximum absorbance around 750 nm ($\varepsilon \approx 350\ L\ mol^{-1}\ cm^{-1}$) with a low energy shoulder around 950 nm ($\varepsilon \approx 220\ L\ mol^{-1}\ cm^{-1}$). The absorbances at 750 and 950 nm are attributed to $d_{xz} \approx d_{yz} \rightarrow d_{z^2}$ and $d_{x^2-y^2} \rightarrow d_{z^2}$ transitions, respectively [274–276]. Based on the absorption spectra, it was concluded that $[Cu^{II}(bpy)_2Br]^+$ cations in DMF are distorted trigonal bipyramidal, which was consistent with the solid state X-ray studies [245].

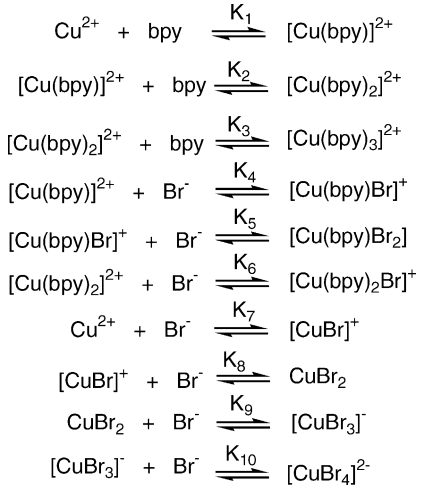

Scheme 14. Equilibrium reactions for ternary Cu^{2+} complexes with 2,2′-bipyridine and bromide anions.

Table 9
Electronic absorption data (vis–NIR) for $Cu^{II}Br_2$ complexes with dNbpy

Complex	Solvent	λ_{max} (nm) (ε[a], L mol^{-1} cm^{-1})		
$[Cu^{II}(dNbpy)Br_2]$	CH_3CN		736 (242)	493 (900)
	MA		721 (232)	512 (899)
	MMA		695 (231)	517 (882)
	BA		700 (249)	521 (930)
	Styrene		735sh (240)	525 (900)
	Toluene		730sh (230)	530 (890)
$[Cu^{II}(dNbpy)_2Br]^+[Br]^-$	CH_3CN	933sh (230)	750 (350)	
	MeOH	930sh (221)	753 (356)	
$[Cu^{II}(dNbpy)_2Br]^+[PF_6]^-$	CH_3CN	950sh (175)	745 (332)	
	MeOH	922sh (190)	744 (352)	
	Toluene	1000sh (160)	745 (320)	
$[Cu^{II}(dNbpy)_2Br]^+[CF_3SO_3]^-$	CH_3CN	950sh (178)	743 (340)	
	MeOH	950sh (180)	743 (336)	
	Toluene	970sh (180)	750 (330)	

sh: shoulder of an absorption band; MA: methyl acrylate; MMA: methyl methacrylate; BA: butyl acrylate.
[a] Extinction coefficient calculated based on total Cu^{II} concentration.

Additionally, the complexation between $Cu^{II}Br_2$ and dNbpy was investigated in different solvents using UV–vis–NIR spectroscopy [253]. The absorption spectra in the vis–NIR region of $[Cu^{II}(dNbpy)Br_2]$ in both the solid state and solution can be characterized in terms of the absorption bands around 700 and 500 nm (Fig. 16). The extinction coefficients in different solvents, including the typical monomers used in ATRP, are given in Table 9. The maximum absorbance around 500 nm ($\varepsilon \approx 900$ L mol^{-1} cm^{-1}) is characteristic of a ligand to metal charge transfer (LMCT) from a bromine to the Cu^{II} center [277–279]. The presence of this charge transfer band in the visible region has been reported for several systems with $Cu^{II}N_2Br_2$ chromophores [280–283], and has been assigned to a square planar arrangement around Cu^{II} center [284,285]. This is consistent with the solid state X-ray structure of $[Cu^{II}(dNbpy)Br_2]$ complex discussed in the previous section. Recognition of this kind of transition further demonstrated the importance of the π-bonding of the halogen ligands in square planar and tetrahedral Cu^{II} complexes [286]. The maximum absorbance near 700 nm ($\varepsilon \approx 230$ L mol^{-1} cm^{-1}) corresponds to the d–d transition. It is characteristic of tetrahedral and square planar Cu^{II} complexes [287]. The similarity of the absorption spectra in the solid state and solution suggests that the geometry of the complex remains unchanged upon dissolution. However, the absorption maxima around 500 nm is solvent dependent. When compared with the solid state, a *blue shift* is observed in the polar and a *red shift* in the non-polar medium. The shift of λ_{max} can also be related to the dielectric constant of the solvent. Generally, for the solvents investigated in this study, the higher the dielectric constant of the solvent, the lower the λ_{max} for LMCT band. This phenomenon has previously been observed for a variety of transition metal complexes [223,288–291] and can be explained in terms of energy localization on bromine ligands. In a polar medium, the Cu–Br bond lengths are more elongated, the electrons more localized around bromine and thus a higher energy (lower λ_{max}) is required for the LMCT transition. On the other hand, in a non-polar medium, the Cu–Br bond lengths are shorter, the electrons around bromine are more delocalized, and consequently, the LMCT transition occurs at a lower energy (higher λ_{max}).

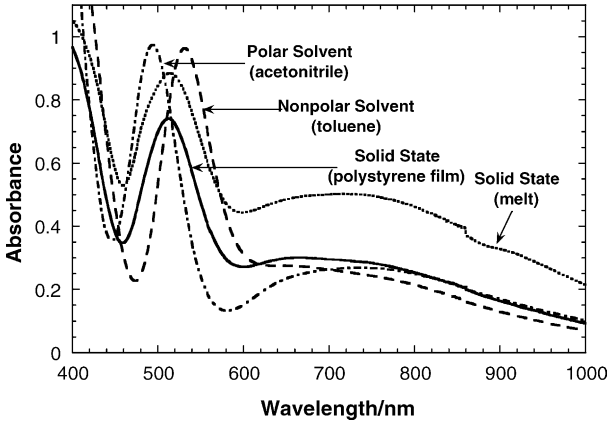

Fig. 16. Absorption spectra (vis–NIR) of $[Cu^{II}(dNbpy)Br_2]$.

As indicated in Fig. 17, the absorption spectrum of $[Cu^{II}(dNbpy)Br_2]$ in methyl methacrylate changes on the addition of dNbpy ligand. The absorbance at 490 nm completely disappears when 1 eq. of dNbpy is added. The disappearance of the 490 nm absorption peak is accompanied by the formation of another absorption peak at 750 nm with a shoulder centered around 950 nm. The final spectrum in Fig. 17, which does not change on further addition of dNbpy ligand, is typical for a distorted trigonal bipyramidal $[CuN_4X]^+$ chromophore [292]. This data suggest that $[Cu^{II}(dNbpy)Br_2]$ displaces $[Br]^-$ anion in the presence of dNbpy to yield $[Cu^{II}(dNbpy)_2Br]^+[Br]^-$ complex (Scheme 15). The thermodynamic data for this equilibrium reaction are summarized in Table 10. The equilibrium constant at room temperature increases as the dielectric constant of the medium increases. The reaction is exothermic in all solvents, as in-

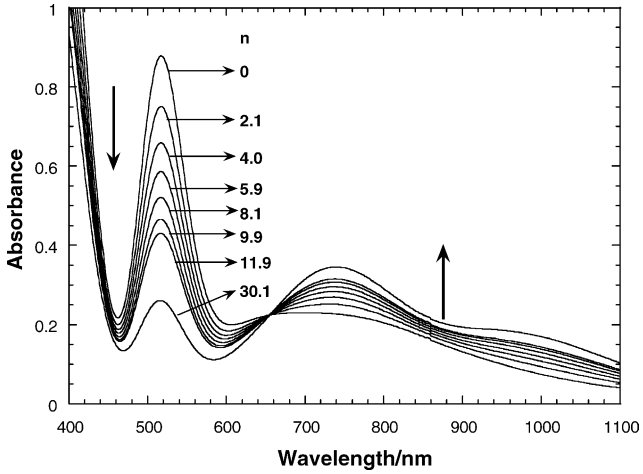

Fig. 17. Addition of n equivalents of dNbpy to $[Cu^{II}(dNbpy)Br_2]$ in MMA at 25 °C, $[Cu^{II}(dNbpy)Br_2]_0 = 1.0 \times 10^{-3}$ M.

dicated by the negative ΔH° values. Similarly, ΔS° values are also negative. The polar medium favors the formation of the $[Cu^{II}(dNbpy)_2Br]^+[Br]^-$ complex because the charge on $[Cu^{II}(dNbpy)_2Br]^+$ cation and $[Br]^-$ anion can be stabilized. The non-polar medium, on the other hand, favors the formation of the neutral $[Cu^{II}(dNbpy)Br_2]$ complex. From the values in Table 10, it can be determined that under the typical reverse ATRP [293] conditions ($T \geq 90$ °C and total copper(II) concentration in the range 1.0×10^{-2} to 1.0×10^{-1} M), $Cu^{II}Br_2$ complex and 2 eq. of dNbpy will predominantly form the neutral $[Cu^{II}(dNbpy)Br_2]$ complex.

Electrospray ionization mass spectrometry (ESI-MS): Complexation between $Cu^{II}Br_2$ and dNbpy was also investigated using ESI-MS [183]. The ESI-MS spectra of the $Cu^{II}Br_2$ complex with 1 eq. of dNbpy in non-polar medium indicated the presence of $[Cu^{II}(dNbpy)_2Br]^+$ and $[Cu^{II}(dNbpy)Br]^+$ cations and $[Cu^{I}Br_2]^-$ and $[Cu^{II}Br_3]^-$ anions. When 2 eq. of dNbpy were used, an additional peak due to $[Cu^{II}(dNbpy)Br_3]^-$ anions was detected. Based on the relative intensities of the different peaks, we concluded that one possible structure of the complex in solution was $[Cu^{II}(dNbpy)_2Br]^+[Cu^{II}Br_3]^-$. This result is inconsistent with the solid state X-ray structure of $[Cu^{II}(dNbpy)Br_2]$ and UV–vis spectrophotometric studies. However, the intensity of $[Cu^{II}(dNbpy)Br_2]$ complex would be relatively low in the ESI-MS because of the absence of charge in the complex. This could lead to the wrong conclusion about the most probable structure in solution.

Extended X-ray absorption fine structure spectroscopy (EXAFS): The results of the EXAFS analysis of $Cu^{II}Br_2$ complex with 2 eq. of dNbpy in methyl acrylate (Table 11) indicated that the coordination sphere around Cu^{II} center consists of 1.4 N atoms at the distance of 2.01 Å and 1.5 Br atoms at the distance of 2.37 Å. In toluene, the average Cu^{II}–N and Cu^{II}–Br distances did not change significantly, and the coordination numbers of nitrogen and bromine increased to 1.8 and 2.1, respectively. In more polar solvent, such as methanol, the coordination number of the nitrogen increased even further to 2.8, and that of the bromine decreases to 0.6. Furthermore, the decrease in the bromine coordination number was accompanied by an increase in the average Cu^{II}–Br bond distance from 2.37 to 2.43 Å. In non-polar medium such as toluene and methyl acrylate, the results of the EXAFS measurements are consistent with a neutral $[Cu^{II}(dNbpy)Br_2]$ complex discussed above [253]. In polar medium, on the other hand, $[Cu^{II}(dNbpy)_2Br]^+[Br]^-$ is preferred.

Electron spin resonance (ESR): Electron spin resonance (ESR) has been widely used to study the structures of copper(II) complexes in solution and solid state

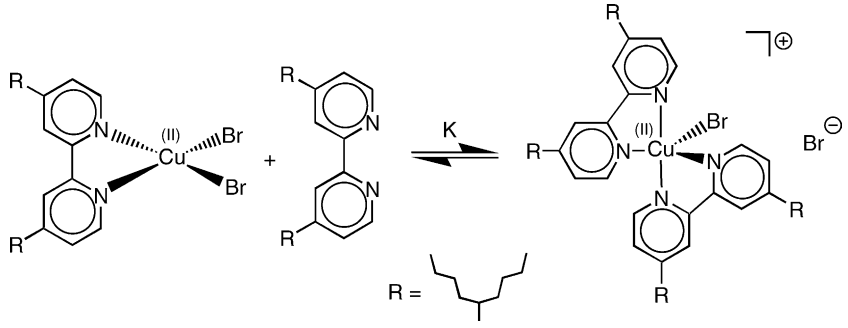

Scheme 15. Proposed equilibrium for the reaction between $[Cu^{II}(dNbpy)Br_2]$ and dNbpy.

Table 10
Thermodynamic data for equilibrium in Scheme 15 in different solvents

Solvent	Dielectric constant, ε	K_{298} (L mol^{-1})	K_{363} (L mol^{-1})	ΔH° (kJ mol^{-1})	ΔS° (J K^{-1} mol^{-1})
Toluene	2.38[20]	13.4 ± 0.54	0.810 ± 0.032	−39.2 ± 3.4	−110 ± 5.6
Styrene	2.47[20]	15.5 ± 0.93	1.13 ± 0.068	−36.0 ± 2.3	−98.1 ± 7.6
n-BA	5.63[20]	78.0 ± 3.1	6.93 ± 0.27	−33.7 ± 3.1	−76.7 ± 6.9
MMA	6.32[30]	72.0 ± 2.9	2.02 ± 0.081	−49.4 ± 3.1	−130 ± 7.4
MA	7.03[30]	251 ± 12.6	0.847 ± 0.042	−78.7 ± 3.9	−218 ± 11

Table 11
Structural parameters of $Cu^{II}Br_2$ complex with 2 eq. of dNbpy ligand, determined by EXAFS measurements under ambient conditions at the Cu K- and Br K-edge

Solvent	Backscattering	*N*	*r* (Å)	*σ* (Å)	ΔE_0 (eV)	*k* ($Å^{-1}$)	Fit index
MA	Cu—N	1.4	2.01	0.071	17.2	4.0–13.7	29.1
	Cu—Br	1.5	2.37	0.071			
	Cu—C	2.0	2.94	0.049			
	Br—Cu	0.9	2.37	0.059	13.5	4.1–14.0	31.6
Toluene	Cu—N	1.8	2.03	0.051	15.0	4.1–15.1	20.1
	Cu—Br	2.1	2.37	0.074			
	Cu—C	1.6	2.93	0.049			
	Br—Cu	1.1	2.35	0.062	18.8	4.2–14.1	16.5
MeOH	Cu—N	2.8	2.03	0.071	17.8	4.2–14.8	27.0
	Cu—Br	0.6	2.43	0.063			
	Br—Cu	0.30	2.42	0.067	19.4	4.2–14.1	56.9

[294–296]. This technique was also used to investigate structural features of Cu^{II} complexes with dNbpy (4,4′-di(5-nonyl)-2,2′-bipyridine) and d*n*Nbpy (4,4′-di-*n*-nonyl-2,2′-bipyridine) ligands in methyl isobutyrate (MIB) and toluene [297]. Additionally, ESR studies were also performed in ATRP of styrene, methyl acrylate and methyl methacrylate [298–300].

The results of the ESR studies indicated that $Cu^{II}Br_2$ in the presence of 1 or 2 eq. of d(*n*)Nbpy ligand in relatively non-polar medium such as MIB and toluene predominantly formed the neutral Cu^{II}(d(*n*)Nbpy)Br_2 complex (Fig. 18). This was consistent with the X-ray structure of [Cu^{II}(dNbpy)Br_2] and UV–vis spectrophotometric studies discussed above. However, the ESR spectrum of the Cu^{II} complex that was generated during bromine atom transfer between $[Cu^{I}(dnNbpy)_2]^+[Cu^{I}Br_2]^-$ and ethyl 2-bromoisobutyrate (EBriB) in MIB was $[Cu^{II}(dnNbpy)_2Br]^+[Cu^{I}Br_2]^-$ and not [Cu^{II}(dNbpy)Br_2]. The same species were also formed in solutions of [Cu^{II}(d*n*Nbpy)Br_2] containing excess $[Cu^{I}(dnNbpy)_2]^+[Cu^{I}Br_2]^-$. The equilibrium constant for the reaction between [Cu^{II}(d*n*Nbpy)Br_2] and $[Cu^{I}(dnNbpy)_2]^+[Cu^{I}Br_2]^-$ to generate $[Cu^{II}(dnNbpy)_2Br]^+$ $[Cu^{I}Br_2]^-$ was estimated in methyl isobutyrate at 23 °C to be $K \geq 100\ M^{-1/2}$.

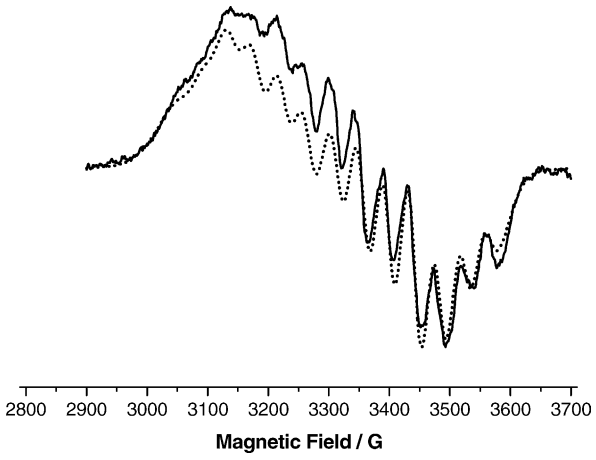

Fig. 18. ESR spectra of 0.5 mM $CuBr_2$ and 0.5 mM d*n*Nbpy in MIB at 23 °C (solid line) and simulation (dotted line).

4.2. Tridentate ligands

4.2.1. DETA and PMDETA

Copper(II) complexes with diethylenetriamine (DETA) and *N*,*N*,*N*′,*N*″,*N*″-pentamethyldiethylenetriamine (PMDETA) are well studied and documented in the literature sources. Generally, DETA and PMDETA coordinate to the copper(II) center as tridentate ligands. $Cu^{II}X_2$ (X = halide or pseudohalide) complexes with PMDETA ligand are typically neutral with the general formula [Cu^{II}(PMDETA)X_2], as observed in the crystal structure of [Cu^{II}(PMDETA)Cl_2] [301] and [Cu^{II}(PMDETA)Br_2] [254]. Typically, pentacoordinated copper(II) complexes have trigonal bipyramidal or square pyramidal geometry, both configurations being energetically equally favorable [302]. In the case of trigonal bipyramidal geometry Cu^{II}–X bond lengths in CuN_3X_2 chromophores are of equal length. On the other hand, the existence of square pyramidal geometry is usually indicated by apical elongation of Cu^{II}–X bond by about 0.1–0.2 Å when compared to the basal Cu^{II}–X bond distance. The Cu^{II}–Cl bond lengths in [Cu^{II}(PMDETA)Cl_2] are $Cu^{II}–Cl_{basal}$ = 2.292(7) Å and $Cu^{II}–Cl_{apical}$ = 2.480(6) Å, indicating that the complex has square pyramidal geometry. The addition of Cu^{I}Cl to [Cu^{II}(PMDETA)Cl_2] complex resulted in the formation of [Cu^{II}(PMDETA)Cl_2(Cu^{I}Cl)] [301] (Scheme 16) with even more pronounced square pyramidal geometry of copper(II) center, as indicated by an increase in the difference between basal and apical copper(II) chlorine bond ($Cu^{II}–Cl_{basal}$ = 2.283(3) Å and $Cu^{II}–Cl_{apical}$ = 2.671(4) Å).

Fig. 19 shows the molecular structure of [Cu^{II}(PMDETA)Br_2] which precipitated from the ATRP of methyl acrylate catalyzed by Cu^{I}Br/PMDETA [254]. Similar to [Cu^{II}(PMDETA)Cl_2], the complex has a square pyramidal coordination sphere with three nitrogens and one bromide situated in the basal plane and the second bromide in the apical position. The Cu^{II}–Br bond length in the apical

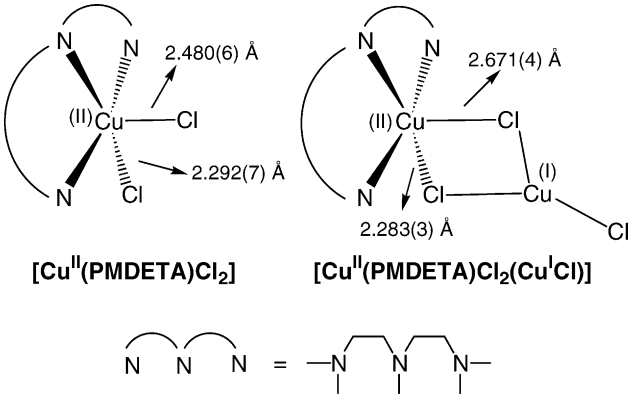

Scheme 16. Apical elongation of Cu^{II}–Cl bond in square pyramidal $[Cu^{II}(PMDETA)Cl_2]$ and $[Cu^{II}(PMDETA)Cl_2(Cu^{I}Cl)]$ complexes.

position (2.6442(9) Å) is much longer than the Cu^{II}–Br bond length in the basal position (2.4462(9) Å). The cleavage of the Cu^{II}–Br bond by the corresponding radical in the deactivation process of the ATRP is therefore expected to occur in the apical position because it is energetically more favorable. Complexation between $Cu^{II}Br_2$ and PMDETA was also investigated using extended X-ray absorption fine structure (EXAFS) [193]. The average Cu^{II}–N bond length determined by EXAFS in Tol/MeOH (2.13 Å), MeOH (2.09 Å) and H_2O (2.06 Å) was in good agreement with the average Cu^{II}–N bond length in $[Cu^{II}(PMDETA)Br_2]$ complex (2.098 Å). However, the average Cu^{II}–Br bond distance in Tol/MeOH (2.42 Å) and MeOH (2.41 Å) was inconsistent with the average bond distance in $[Cu^{II}(PMDETA)Br_2]$ (2.545 Å). The structural features of $Cu^{II}Br_2$ complex with PMDETA determined by EXAFS can be explained in terms of bromide dissociation from $[Cu^{II}(PMDETA)Br_2]$. In Tol/MeOH and MeOH, the EXAFS data suggested the presence of $[Cu^{II}(PMDETA)Br_2]$ and $[Cu^{II}(PMDETA)Br]^+[Br]^-$. In H_2O, additional dissociation of bromide could result in the formation of $[Cu^{II}(PMDETA)]^{2+}[Br]_2^-$. As Cu^{II} complexes prefer pentacoordinated geometry [223], the empty coordination sites in $[Cu^{II}(PMDETA)Br]^+[Br]^-$ and $[Cu^{II}(PMDETA)]^{2+}[Br]_2^-$ are likely occupied by solvent molecules (MeOH or H_2O) (Scheme 17). This was demonstrated in the solid state X-ray structures of related complexes $[Cu^{II}(PMDETA)(H_2O)]^{2+}[ClO_4]_2^-$ [303] and $[Cu^{II}(PMDETA)(H_2O)_2]^{2+}[BF_4]_2^-$ [304]. The substitution of bromide via π-bond formation with monomer is less likely to occur with Cu^{II} complexes because the binding constants are typically very low [305]. However, substitution can potentially occur with functionalized olefins because they can additionally coordinate to the Cu^{II} complexes via functional groups (S, O, N, etc.) [199].

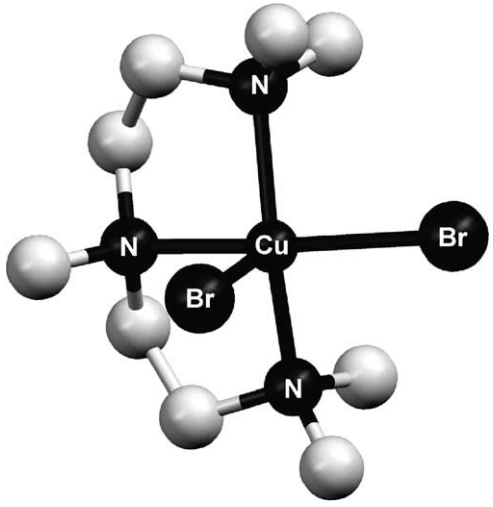

Fig. 19. Molecular structure of $[Cu^{II}(PMDETA)Br_2]$.

In the case of copper(II) complexes with DETA ligand, bridging via halogens or pseudo halogens has been observed in dimeric complexes with the general formula $[Cu^{II}(DETA)X]_2{}^{2+}[Y]_2^-$ (Y = non-coordinating anion). Each copper(II) center in the dimer is distorted square pyramidal in geometry with the apical elongation of Cu^{II}–X bond distance by about 0.1–0.2 Å as seen in $[Cu^{II}(DETA)Br]_2{}^{2+}[ClO_4]_2^-$ [306] (Scheme 18), $[Cu^{II}(DETA)Cl]_2{}^{2+}[ClO_4]_2^-$ [307], $[Cu^{II}(DETA)Cl]_2{}^{2+}[NO_3]_2^-$ [308] and $[Cu^{II}(DETA)(SCN)]_2{}^{2+}[ClO_4]_2^-$ [309]. Additionally, $[Cu^{II}(DETA)]^{2+}$ chromophore can be saturated by neutral ligand as observed in the crystal structure of $[Cu^{II}(DETA)(bimH_2)]^{2+}[ClO_4]_2^-$ ($bimH_2$ = 2,2′-biimidazole) [310].

4.2.2. tpy and tpy derivatives

General structural features of copper(II) complexes with tpy based ligands observed in the solid state are shown in Scheme 19. Copper(II) complexes with tpy based ligands are usually synthesized by the reaction of $Cu^{II}X_2$ (X = halide or pseudohalide) salts with 1 eq. of tpy ligand. In non-aqueous medium, $[Cu^{II}(tpy)X_2]$ are typically isolated as in the case of $[Cu^{II}(tpy)Br_2]$ [311], $[Cu^{II}(tNtpy)Br_2]$ [254] (Fig. 20), $[Cu^{II}(tpy)Cl_2]$ [312], $[Cu^{II}(tpy)F_2]\cdot 3H_2O$ [313], $[Cu^{II}(tpy)(N_3)_2]$ [314] and $[Cu^{II}(tpy)(NCS)_2]$ [311] complexes. In all complexes, Cu^{II} center is coordinated by three nitrogen atoms of tpy ligand and two halogen atoms. Cu^{II}–N bond distances in coordinated tpy ligand are typically unequal and range from 1.95 to 2.05 Å. $[Cu^{II}(tpy)X_2]$ complexes are either trigonal bipyramidal or square pyramidal since both configurations are energetically equally favorable [302]. Typically, the two stereochemistries are distinguished by the Cu^{II}–X bond lengths. In the case when Cu^{II}–X_1 = Cu^{II}–X_2 the complex is usually distorted trigonal bipyramidal as observed in the case of $[Cu^{II}(tpy)Br_2]$ (Cu^{II}–Br = 2.493(1) Å), $[Cu^{II}(tpy)(NCS)_2]$ (Cu^{II}–N = 2.020(7) Å). In the case when Cu^{II}–$X_1 \neq Cu^{II}$–X_2, or apical elongation of one of the Cu^{II}–X bonds, complexes are distorted square pyramidal as observed in $[Cu^{II}(tNtpy)Br_2]$ (Cu^{II}–Br = 2.5276(10) and 2.4071(10) Å), $[Cu^{II}(tpy)Cl_2]$ (Cu^{II}–Cl = 2.231(2) and 2.565(2) Å), $[Cu^{II}(tpy)F_2]\cdot 3H_2O$ (Cu^{II}–F = 1.862(4) and 2.104(5) Å) and $[Cu^{II}(tpy)(N_3)_2]$ (Cu^{II}–N = 1.96(2) and 2.21(2) Å).

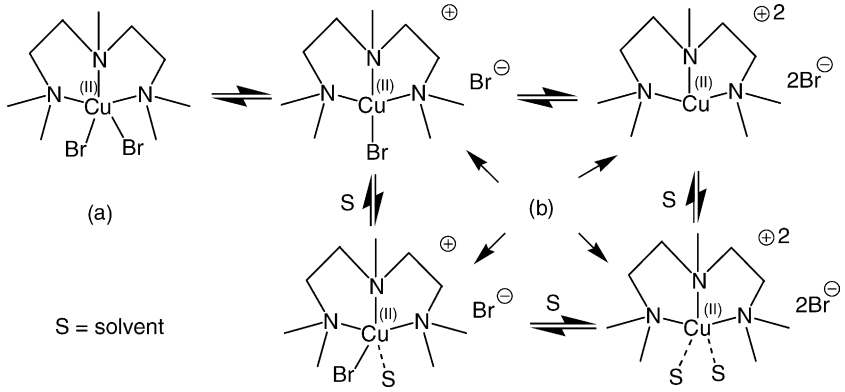

Scheme 17. Proposed structures for $Cu^{II}Br_2$/PMDETA complex in non-polar (a) and polar (b) medium based on EXAFS measurements.

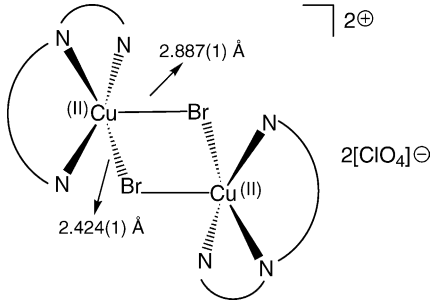

Scheme 18. Basal and apical Cu^{II}—Br bond lengths in $[Cu^{II}(DETA)Br]_2^{2+}[ClO_4]_2^-$ dimer.

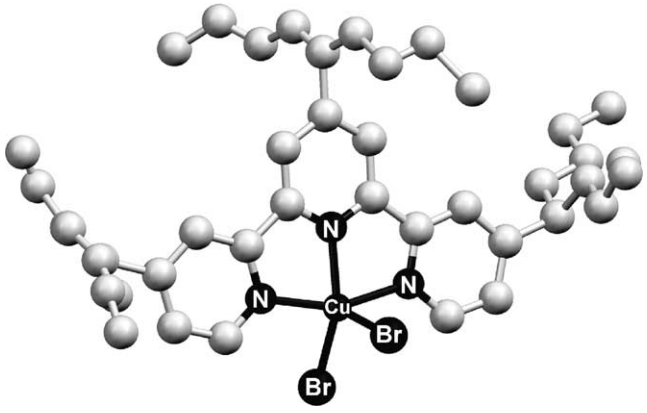

Fig. 20. Molecular structure of $[Cu^{II}(tNtpy)Br_2]$.

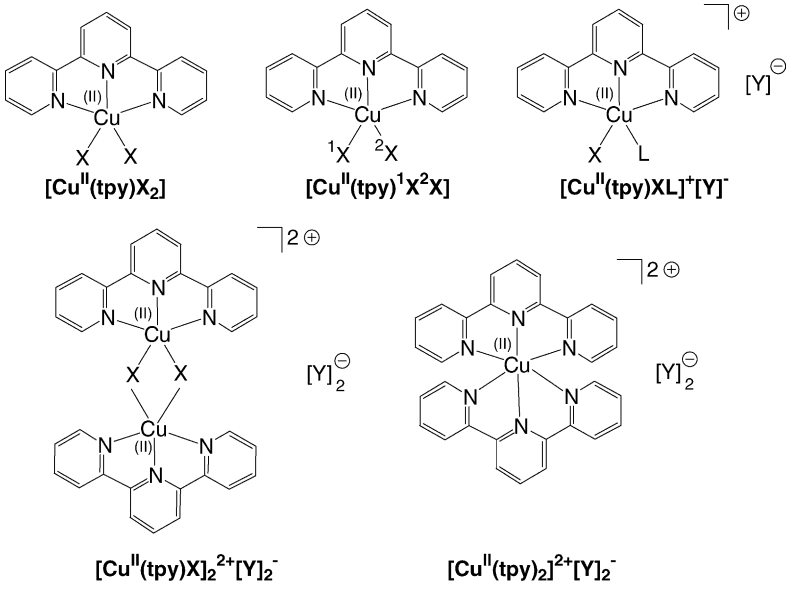

Scheme 19. General structures of copper(II) complexes with tpy ligand.

$[Cu^{II}(tpy)X_2]$ complexes can be reacted with different halide or pseudohalide anions resulting in a formation of mixed $[Cu^{II}(tpy)X^1X^2]$ complexes. This has been demonstrated in the case of distorted square pyramidal $[Cu^{II}(tpy)(N_3)(Cl)]$ [315] complex.

When the synthesis of Cu^{II} complexes with tpy ligands is carried in aqueous medium, and in the presence of non-coordinating and coordinating anions, $[Cu^{II}(tpy)(H_2O)X]^+[Y]^-$ and $[Cu^{II}(tpy)(H_2O)X_1]^+[X_2]^-$ complexes are typically formed as observed in the distorted square pyramidal $[Cu^{II}(tpy)(N_3)(H_2O)]^+[NO_3]^-$ [316] and $[Cu^{II}(tpy)(N_3)(H_2O)]^+[PF_6]^-$ complexes [316]. In some cases, bridging via halide anions can occur as demonstrated in $[Cu^{II}(tpy)Cl]_2^{2+}[PF_6]_2^-$ [317,318] and $[Cu^{II}(tpy)Br]_2^{2+}[PF_6]_2^-$ [319].

Lastly, when excess of tpy ligand is used in the synthesis, $[Cu^{II}(tpy)_2]^{2+}$ cations are typically formed as confirmed by the solid state X-ray structures $[Cu^{II}(tpy)_2]^{2+}[Br]_2^-$ [320] and $[Cu^{II}(tpy)_2]^{2+}[PF_6]_2^-$ [321]. $[Cu^{II}(tpy)_2]^{2+}$ cations are typically distorted octahedral in geometry with the Cu^{II}–N bond length ranging from to 1.95 to 2.15 Å.

4.3. Tetradentate ligands

4.3.1. TREN and Me_6TREN

Copper(II) complexes with tetradentate nitrogen based ligands tris[2-aminoethyl]amine (TREN) and tris[2-(dimethylamino)ethyl]amine (Me_6TREN) are typically pentacoordinated in which the copper(II) center is coordinated by four nitrogen atoms of TREN or Me_6TREN ligand and a donor atom from monodentate neutral or charged ligand. The complexes are typically prepared by reacting Cu^{II} salts with 1 eq. of the ligand.

In the case of $Cu^{II}X_2$ salts (X = halide or pseudohalide), $[Cu^{II}(TREN \text{ or } Me_6TREN)X]^+[X]^-$ complexes are typically formed as observed in $[Cu^{II}(Me_6TREN)Br]^+[Br]^-$ [254,322] (Fig. 21) and $[Cu^{II}(TREN)(NCS)]^+[NCS]^-$ [323] complexes. $[Cu^{II}(Me_6TREN)Br]^+$ cations in $[Cu^{II}(Me_6TREN)Br]^+[Br]^-$ are distorted trigonal bipyramidal in geometry ($Cu^{II}–N_1 = Cu^{II}–N_2 = Cu^{II}–N_3 = 2.143$ Å, $Cu^{II}–N_4 = 2.069$ Å and $Cu^{II}–Br = 2.393$ Å) [322]. The same geometry was also observed in $[Cu^{II}(TREN)(NCS)]^+$ cations ($Cu^{II}–N_{AV} = 2.020$ Å and $Cu^{II}–N(NCS) = 2.162$ Å) [323].

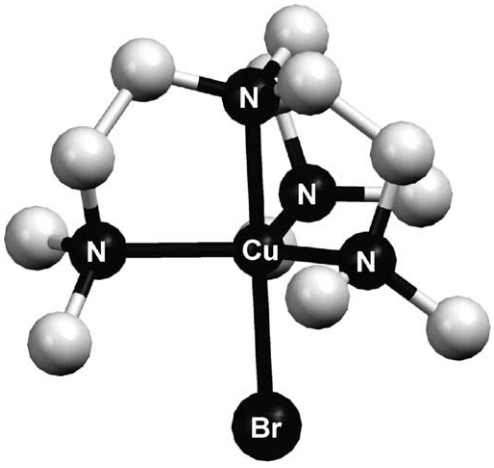

Fig. 21. Molecular structure of $[Cu^{II}(Me_6TREN)Br]^+$ cation in $[Cu^{II}(Me_6TREN)Br]^+[Br]^-$ [322].

When $Cu^{II}Y_2$ salts ($Y = PF_6^-, CF_3SO_3^-, ClO_4^-$, etc.) are used in the synthesis, the isolated complexes typically have the general formula $[Cu^{II}(TREN \text{ or } Me_6TREN)(L)]^{2+}[Y]_2^-$, where L is the neutral monodentate ligand. The coordination of a neutral ligand to $[Cu^{II}N_4]^{2+}$ chromophores has been observed in $[Cu^{II}(TREN)(NH_3)]^{2+}[ClO_4]_2^-$ [324] and $[Cu^{II}(Me_6TREN)(H_2O)]^{2+}[ClO_4]_2^-$ [233] complexes. The neutral ligand can be easily displaced by halide anions, yielding the corresponding $[Cu^{II}(TREN \text{ or } Me_6TREN)X]^+[Y]^-$ complexes as seen for example in the synthesis of $[Cu^{II}(Me_6TREN)Cl]^+[ClO_4]^-$ complex [229].

Complexation between $Cu^{II}Br_2$ and Me_6TREN was also investigated in solution using EXAFS [254]. In methanol, the EXAFS spectrum of the Cu K-edge was reasonably well fit assuming the structural model that included on average 3.2 nitrogen atoms at the distance of 2.13 Å and 1.4 bromine atoms at the distance of 2.38 Å. This data are consistent with $[Cu^{II}(Me_6TREN)Br]^+[Br]^-$ complex discussed above. In more polar solvent such as H_2O, a significant decrease in the coordination number of bromine was observed. This result pointed to the bromide dissociation and formation of $[Cu^{II}(Me_6TREN)(H_2O)]^+[Br]^-$ complex.

4.3.2. TETA and HMTETA

Copper(II) complexes with triethylenetetramine (TETA) and 1,1,4,7,10,10-hexamethyltriethylenetetramine (HMTETA) similarly to TREN and Me_6TREN prefer pentacoordinated geometry in which copper(II) center is coordinated by four nitrogen atoms of TETA or HMTETA ligand and the donor atom of a neutral or charged monodentate ligand. Typically, complexes are square pyramidal in geometry as observed in $[Cu^{II}(TETA)(NCS)]^+[NCS]^-$ [325], $[Cu^{II}(HMTETA)Cl]^+[ClO_4]^-$ [230] and $[Cu^{II}(HMTETA)Br]^+[Br]^-$ [254] (Fig. 22) complexes. Molecular structure of $[Cu^{II}(HMTETA)Br]^+[Br]^-$ indicated that the complex has a distorted square pyramidal geometry ($Cu^{II}–N = 2.082(12)$, 2.082(12), 2.103(10) and 2.167(17) Å and $Cu^{II}–Br = 2.6027(18)$ Å). The distance between the bromine anion and the Cu^{II} center in $[Cu^{II}(HMTETA)Br]^+[Br]^-$ is 4.645 Å, which indicates that the anion is non-coordinating.

4.3.3. CYCLAM and Me_4CYCLAM

Cyclic tetradentate 1,4,8,11-tetraazacyclotetradecane (CYCLAM) and 1,4,8,11-tetraaza-1,4,8,11-tetramethylcyclotetradecane (Me_4CYCLAM) ligands readily form complexes with copper(II) ions which are typically pentacoordinated, the fifth coordination site usually being occupied by either neutral or charged monodentate ligand. Due to the steric effects of the cyclic ligand, the complexes are typically square pyramidal as observed in the

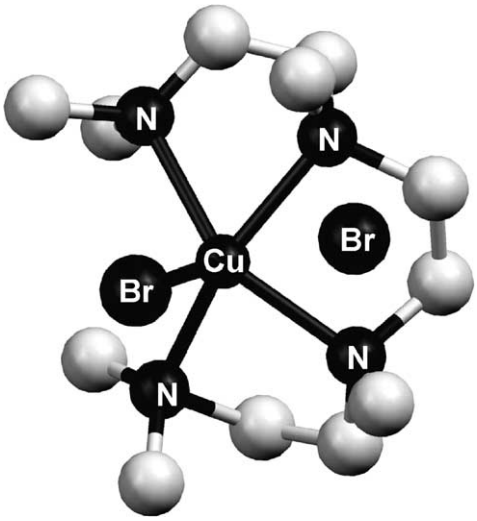

Fig. 22. Molecular structure of $[Cu^{II}(HMTETA)Br]^+[Br]^-$.

X-ray structures of $[Cu^{II}(Me_4CYCLAM)Cl]^+[Cl]^-\cdot 1.5H_2O$ [326], $[Cu^{II}(Me_4CYCLAM)(H_2O)]^{2+}[NO_3]_2^-\cdot H_2O$ [326], $[Cu^{II}(CYCLAM)Cl]^+[Cl]^-$ [327], $[Cu^{II}(CYCLAM)Br]^+[Br]^-$ [327] and $[Cu^{II}(Me_4CYCLAM)Br]^+[Br]^-$ [254]. Additionally, a neutral octahedral $[Cu^{II}(CYCLAM)(SPh)_2]$ complex has also been synthesized and characterized [328].

Fig. 23 shows the molecular structure of $[Cu^{II}(Me_4CYCLAM)Br]^+[Br]^-$ which was isolated from ATRP [254]. The $[Cu^{II}(Me_4CYCLAM)Br]^+[Br]^-$ complex is square pyramidal in geometry and the Cu^{II}–Br bond length is 2.8092(6) Å. The shortest distance between the $[Br]^-$ anion and $[Cu^{II}(Me_4CYCLAM)Br]^+$ cation is 4.349 Å, which indicates no substantial interaction and rules out the possibility for semicoordination in the solid state.

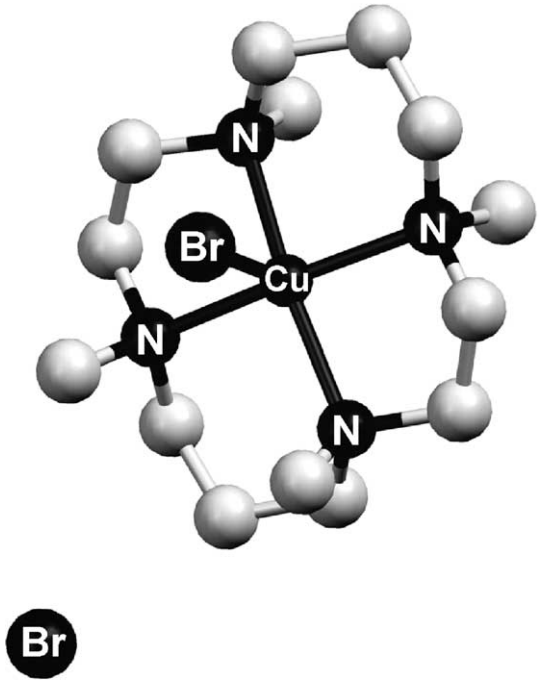

Fig. 23. Molecular structure of $[Cu^{II}(Me_4CYCLAM)Br]^+[Br]^-$.

Table 12
Comparison of the Cu^{II}–Br bond length in the Cu^{II} complexes with the deactivation rate constant in the ATRP equilibrium

Complex	Cu^{II}–Br (Å)	k_d ($M^{-1}\,s^{-1}$)	Reference
$[Cu^{II}(Me_6TREN)Br]^+[Br]^-$	2.393(3)	1.4×10^{7} [a]	[322,330]
$[Cu^{II}(dNbpy)Br]^+[Cu^{I}Br_2]^-$	2.426(3)	2.5×10^{7} [a]	[330]
$[Cu^{II}(tNtpy)Br_2]$	2.5276(10)	4.1×10^{5} [a]	[331]
	2.4071(10)		
$[Cu^{II}(PMDETA)Br_2]$	2.6442(9)	6.1×10^{6} [a]	[330]
	2.4462(9)		
$[Cu^{II}(Me_4CYCLAM)Br]^+[Br]^-$	2.8092(6)	2.0×10^{4} [b]	[228]

Only the bond lengths of the cations are considered.
[a] Rate constant measured in CH_3CN at 75 °C using 1-phenylethyl radical.
[b] Rate constant estimated by the degree of polymerization of poly(styrene) formed by initiation with AIBN in the presence of $CuBr_2$/cyclam and 1-phenylethyl bromide.

5. Correlating Cu^{II}–Br bond length and deactivation rate constant (k_d)

The structures of the Cu^{I} and Cu^{II} complexes that are involved in the ATRP equilibrium play an important role in determining the overall activity of the catalyst. Previously, this activity has been correlated with properties such as redox potential [329] and more recently the activation and deactivation rate constants [228,330–335]. Additionally, factors such as the polarity of the monomers and reaction medium are also related to the catalyst activity. The simplest structural parameter that can be correlated with the kinetics of the ATRP deactivation process is the Cu^{II}–Br bond length. The strength of this bond can be used as a crude estimate to evaluate the deactivation rate constant, which is responsible for the control in the ATRP systems. Table 12 shows the comparison between the Cu^{II}–Br bond length and the deactivation rate constant for the Cu^{II} complexes with Me_6TREN, dNbpy, tNtpy, PMDETA and Me_4CYCLAM. As indicated in the table, there is no direct correlation between the length of the Cu^{II}–Br bond and the deactivation rate constant. It appears that the weaker or longer Cu^{II}–Br bond length is not the only factor that effects the deactivation rate constant. The structural reorganization of the Cu^{II} complex upon bromine abstraction by the corresponding radical is another important process that needs to be taken into account. For example, the structural features of $[Cu^{I}(Me_6TREN)]^+[ClO_4]^-$ (Fig. 8) and $[Cu^{II}(Me_6TREN)Br]^+[Br]^-$ (Fig. 21) complexes, which mimic activator and deactivator in the ATRP, respectively, reveal that bromine abstraction by $[Cu^{I}(Me_6TREN)]^+$ cation slightly changes the structure of the resulting $[Cu^{II}(Me_6TREN)Br]^+$ cation. More precisely, Cu^{II} cation moves inside Me_6TREN cavity by 0.13 Å and Cu^{II}–N bond lengths slightly elongate by approximately 0.02 Å. This small structural reorganization can explain the fact that the deactivation rate constant for 1-phenylethyl ra-

dial ($k_d = 1.4 \times 10^7\ M^{-1}\ s^{-1}$) is relatively large despite very short Cu^{II}–Br bond length (2.393(3) Å).

6. Conclusions

In conclusion, structural features of Cu^{I} and Cu^{II} complexes with bidentate, tridentate and tetradentate nitrogen based ligands commonly used in the ATRP were extensively reviewed and discussed based on several spectroscopic techniques. They included solid state X-ray crystallography, extended X-ray absorption fine structure (EXAFS), electrospray ionization mass spectrometry (ESI-MS), NMR and UV–vis spectrometry. The structures were found to depend on the complexing ligand, solvent and temperature. Generally, copper(I) complexes were found to be predominantly four coordinated. On the other hand, the coordination number of copper(II) complexes was found to be either four or five depending on the complexing ligand. Structural studies are a continuous part of the future developments in the field of ATRA/ATRP.

Acknowledgement

The authors would like to acknowledge the support from the National Science Foundation (CHE-00-96601 and 04-05627) as well as ATRP and CRP Consortia at Carnegie Mellon University.

References

[1] D.P. Curran, Synthesis 7 (1988) 489.
[2] D.P. Curran, Synthesis 6 (1988) 417.
[3] M.S. Kharasch, E.V. Jensen, W.H. Urry, Science 102 (1945) 128.
[4] M.S. Kharasch, E.V. Jensen, W.H. Urry, J. Am. Chem. Soc. 67 (1945) 1626.
[5] D.H. Hey, W.A. Waters, Chem. Rev. 21 (1937) 169.
[6] M.S. Kharasch, H. Engelmann, F.R. Mayo, J. Org. Chem. 2 (1938) 288.
[7] D. Bellus, Pure Appl. Chem. 57 (1985) 1827.
[8] J.H. Udding, C.J.M. Tuijp, N.A. van Zanden, H. Hiemstra, W.N. Speckamp, J. Org. Chem. 59 (1994) 1993.
[9] H. Nagashima, N. Ozaki, M. Ishii, J. Seki, M. Washiyama, K. Itok, J. Org. Chem. 58 (1993) 464.
[10] M. Asscher, D. Vofsi, J. Chem. Soc. (1963) 1887.
[11] M. Benedetti, L. Forti, F. Ghelfi, U.M. Pagnoni, R. Ronzoni, Tetrahedron 53 (1997) 14031.
[12] G.M. Lee, N. Parvez, S.M. Weinreb, Tetrahedron 44 (1988) 4671.
[13] R.K. Freidlina, F.K. Velichko, Synthesis 3 (1977) 145.
[14] H. Matsumoto, T. Nakano, Y. Nagai, Tetrahedron Lett. 51 (1973) 5147.
[15] W.J. Bland, R. Davis, J.L.A. Durrant, J. Organomet. Chem. 260 (1984) C75.
[16] Y. Sasson, G.L. Rempel, Synthesis (1975) 448.
[17] D.M. Grove, G. Van Koten, A.H.M. Verschuuren, J. Mol. Catal. 45 (1988) 169.
[18] M. Hajek, P. Silhavy, J. Malek, Collection Czechoslov. Chem. Commun. 45 (1980) 3488.
[19] M. Hajek, P. Silhavy, J. Malek, Collection Czechoslov. Chem. Commun. 45 (1980) 3502.
[20] E. Steiner, P. Martin, D. Bellius, Helv. Chim. Acta 65 (1982) 983.
[21] J.O. Metzger, R. Mahler, Angew. Chem. Int. Ed. Engl. 34 (1995) 902.
[22] L. Forti, F. Ghelfi, U.M. Pagnoni, Tetrahedron Lett. 37 (1996) 2077.
[23] F. Bellesia, L. Forti, F. Ghelfi, U.M. Pagnoni, Synth. Commun. 27 (1997) 961.
[24] L. Forti, F. Ghelfi, E. Libertini, U.M. Pagnoni, E. Soragni, Tetrahedron 53 (1997) 17761.
[25] J.A. Baban, B.P. Roberts, J. Chem. Soc., Perkin Trans. 1 (1981) 161.
[26] T. Caronna, A. Citterio, M. Ghirardini, F. Minisci, Tetrahedron 33 (1977) 793.
[27] F. Minisci, Acc. Chem. Res. 8 (1975) 165.
[28] M. Asscher, D. Vofsi, J. Chem. Soc. (1964) 4962.
[29] J. Sinnreich, M. Asscher, J. Chem. Soc., Perkin Trans. 1 (1972) 1543.
[30] N. Kamigata, H. Sawada, M. Kobayashi, J. Org. Chem. 48 (1983) 3793.
[31] E. Block, M. Aslam, V. Eswarakrishnan, K. Gebreyes, J. Hutchinson, R.S. Iyer, J.A. Laffitte, J. Am. Chem. Soc. 108 (1986) 4568.
[32] Y. Amiel, J. Org. Chem. 39 (1974) 3867.
[33] W.E. Truce, G.C. Wolf, J. Org. Chem. 36 (1971) 1727.
[34] Y. Pietrasanta, G. Rigal, C.R. Acad. Sci., Paris 274 (1972) 2056.
[35] M. Julia, L. Sasussine, G.I. Thuillier, J. Organomet. Chem. 174 (1979) 359.
[36] F. De Campo, D. Lastecoures, J.-B. Verlhac, J. Chem. Soc., Perkin Trans. 14 (2000) 575.
[37] R.A. Gossage, L.A. Van de Kuil, G. Van Koten, Acc. Chem. Res. 31 (1998) 423.
[38] D.P. Curran, in: B.M. Trost, I. Flemming (Eds.), Comprehensive Organic Synthesis, Pergamon Press, New York, 1992, p. 715.
[39] A.J. Clark, Chem. Soc. Rev. 31 (2002) 1.
[40] M. Asscher, D. Vofsi, J. Chem. Soc. (1961) 2261.
[41] K. Matyjaszewski, T.P. Davis (Eds.), Handbook of Radical Polymerization, Wiley, Hoboken, 2002.
[42] K. Matyjaszewski (Ed.), Controlled Radical Polymerization, ACS Symposium Series, Washington, DC, 1998.
[43] K. Matyjaszewski (Ed.), Controlled/Living Radical Polymerization: Progress in ATRP, NMP and RAFT, ACS Symposium Series, Washington, DC, 2000.
[44] K. Matyjaszewski (Ed.), ACS Symposium Series, vol. 854, 2003, 688 pp.
[45] K. Matyjaszewski, J. Xia, Chem. Rev. 101 (2001) 2921.
[46] M. Kamigaito, T. Ando, M. Sawamoto, Chem. Rev. 101 (2001) 3689.
[47] J.-S. Wang, K. Matyjaszewski, J. Am. Chem. Soc. 117 (1995) 5614.
[48] K. Matyjaszewski, Chem. Eur. J. 5 (1999) 3095.
[49] T.E. Patten, Science 272 (1996) 866.
[50] A. Goto, T. Fukuda, Prog. Polym. Sci. 29 (2004) 329.
[51] K. Matyjaszewski, J. Macromol. Sci., Pure Appl. Chem. A 34 (1997) 1785.
[52] K. Matyjaszewski, ACS Symp. Ser. 685 (1998) 258.
[53] K. Matyjaszewski, B.E. Woodworth, Macromolecules 31 (1998) 4718.
[54] K. Matyjaszewski, Macromolecules 32 (1999) 9051.
[55] K. Matyjaszewski, Macromol. Symp. 183 (2002) 71.
[56] K. Matyjaszewski, Macromolecules 35 (2002) 6773.
[57] K. Matyjaszewski, Macromol. Symp. 182 (2002) 209.
[58] T. Pintauer, B. McKenzie, K. Matyjaszewski, ACS Symp. Ser. 854 (2003) 130.
[59] D.A. Singleton, D.T. Nowlan III, N. Jahed, K. Matyjaszewski, Macromolecules 36 (2003) 8609.
[60] H. Fischer, J. Polym. Sci., Part A: Polym. Chem. 37 (1999) 1885.
[61] H. Fischer, Chem. Rev. 101 (2001) 3581.
[62] T.E. Patten, K. Matyjaszewski, Acc. Chem. Res. 32 (1999) 895.

[63] V. Coessens, T. Pintauer, K. Matyjaszewski, Prog. Polym. Sci. 26 (2001) 337.
[64] J.P. Claverie, R. Soula, Prog. Polym. Sci. 28 (2003) 619.
[65] K.A. Davis, K. Matyjaszewski, Adv. Polym. Sci. 159 (2002) 2.
[66] C. Gao, D. Yan, Prog. Polym. Sci. 29 (2004) 183.
[67] T. Kowalewski, R.D. McCullough, K. Matyjaszewski, Eur. Phys. J. E 10 (2003) 5.
[68] I. Luzinov, S. Minko, V.V. Tsukruk, Prog. Polym. Sci. 29 (2004) 635.
[69] K. Matyjaszewski, P.J. Miller, N. Shukla, B. Immaraporn, A. Gelman, B.B. Luokala, T.M. Siclovan, G. Kickelbick, T. Vallant, H. Hoffmann, T. Pakula, Macromolecules 32 (1999) 8716.
[70] K. Matyjaszewski, D.A. Shipp, J. Qiu, S.G. Gaynor, Macromolecules 33 (2000) 2296.
[71] K. Matyjaszewski, M.J. Ziegler, S.V. Arehart, D. Greszta, T. Pakula, J. Phys. Org. Chem. 13 (2000) 775.
[72] K. Matyjaszewski, Nonlinear Opt. Quant. Opt. 30 (2003) 167.
[73] H. Mori, A.H.E. Mueller, Prog. Polym. Sci. 28 (2003) 1403.
[74] T. Pakula, P. Minkin, K. Matyjaszewski, ACS Symp. Ser. 854 (2003) 366.
[75] T.E. Patten, K. Matyjaszewski, Adv. Mater. 10 (1998) 901.
[76] J. Pyun, K. Matyjaszewski, Chem. Mater. 13 (2001) 3436.
[77] J. Pyun, T. Kowalewski, K. Matyjaszewski, Macromol. Rapid Commun. 24 (2003) 1043.
[78] J. Pyun, J. Xia, K. Matyjaszewski, ACS Symp. Ser. 838 (2003) 273.
[79] J. Qiu, B. Charleux, K. Matyjaszewski, Prog. Polym. Sci. 26 (2001) 2083.
[80] J.-F. Lutz, K. Matyjaszewski, Macromol. Chem. Phys. 203 (2002) 1385.
[81] J.-F. Lutz, B. Kirci, K. Matyjaszewski, Macromolecules 36 (2003) 3136.
[82] J.-F. Lutz, D. Neugebauer, K. Matyjaszewski, J. Am. Chem. Soc. 125 (2003) 6986.
[83] K. Matyjaszewski, D.A. Shipp, J.-L. Wang, T. Grimaud, T.E. Patten, Macromolecules 31 (1998) 6836.
[84] K. Matyjaszewski, V. Coessens, Y. Nakagawa, J. Xia, J. Qiu, S. Gaynor, S. Coca, C. Jasieczek, ACS Symp. Ser. 704 (1998) 16.
[85] K. Matyjaszewski, T.E. Patten, J. Xia, J. Am. Chem. Soc. 119 (1997) 674.
[86] J. Qiu, K. Matyjaszewski, Macromolecules 30 (1997) 5643.
[87] J. Xia, X. Zhang, K. Matyjaszewski, Macromolecules 32 (1999) 3531.
[88] J.-L. Wang, T. Grimaud, K. Matyjaszewski, Macromolecules 30 (1997) 6507.
[89] K.A. Davis, H.-J. Paik, K. Matyjaszewski, Macromolecules 32 (1999) 1767.
[90] K.L. Beers, S. Boo, S.G. Gaynor, K. Matyjaszewski, Macromolecules 32 (1999) 5772.
[91] K.A. Davis, K. Matyjaszewski, Macromolecules 33 (2000) 4039.
[92] K.A. Davis, K. Matyjaszewski, Macromolecules 34 (2001) 2101.
[93] K.A. Davis, K. Matyjaszewski, Chin. J. Polym. Sci. 22 (2004) 195.
[94] T. Grimaud, K. Matyjaszewski, Macromolecules 30 (1997) 2216.
[95] J. Huang, T. Pintauer, K. Matyjaszewski, J. Polym. Sci., Part A: Polym. Chem. 42 (2004) 3285.
[96] K. Matyjaszewski, Y. Nakagawa, C.B. Jasieczek, Macromolecules 31 (1998) 1535.
[97] K. Matyjaszewski, S. Coca, C.B. Jasieczek, Macromol. Chem. Phys. 198 (1997) 4011.
[98] X. Zhang, K. Matyjaszewski, Macromolecules 32 (1999) 1763.
[99] M.J. Ziegler, K. Matyjaszewski, Macromolecules 34 (2001) 415.
[100] H. Shinoda, K. Matyjaszewski, L. Okrasa, M. Mierzwa, T. Pakula, Macromolecules 36 (2003) 4772.
[101] K. Matyjaszewski, S.M. Jo, H.-J. Paik, S. Gaynor, Macromolecules 30 (1997) 6398.
[102] K. Matyjaszewski, S.M. Jo, H.-J. Paik, D.A. Shipp, Macromolecules 32 (1999) 6431.
[103] C. Tang, T. Kowalewski, K. Matyjaszewski, Macromolecules 36 (2003) 1465.
[104] M. Teodorescu, K. Matyjaszewski, Macromolecules 32 (1999) 4826.
[105] D. Neugebauer, K. Matyjaszewski, Macromolecules 36 (2003) 2598.
[106] C. Konak, B. Ganchev, M. Teodorescu, K. Matyjaszewski, P. Kopeckova, J. Kopecek, Polymer 43 (2002) 3735.
[107] Y.A. Kabachii, S.Y. Kochev, L.M. Bronstein, I.B. Blagodatskikh, P.M. Valetsky, Polym. Bull. 50 (2003) 271.
[108] J.A.M. Brandts, P. van de Geijn, E.E. van Faassen, J. Boersma, G. van Kotten, J. Organomet. Chem. 584 (1999) 246.
[109] E. Le Grognec, J. Claverie, R. Poli, J. Am. Chem. Soc. 123 (2001) 9513.
[110] Y. Kotani, M. Kamigaito, M. Sawamoto, Macromolecules 32 (1999) 2420.
[111] K. Matyjaszewski, M. Wei, J. Xia, N.E. McDermott, Macromolecules 30 (1997) 8161.
[112] T. Ando, M. Kamigaito, M. Sawamoto, Macromolecules 30 (1997) 4507.
[113] M. Teodorescu, S. Gaynor, K. Matyjaszewski, Macromolecules 33 (2000) 2335.
[114] V.C. Gibson, R.K. O'Reilly, W. Reed, D.F. Wass, A.J.P. White, D.J. Williams, Chem. Commun. (2002) 1850.
[115] V.C. Gibson, R.K. O'Reilly, D.F. Wass, A.J.P. White, D.J. Williams, Macromolecules 36 (2003) 2591.
[116] V.C. Gibson, R.K. O'Reilly, D.F. Wass, A.J.P. White, D.J. Williams, Dalton Trans. (2003) 2824.
[117] M. Kato, M. Kamigaito, M. Sawamoto, T. Higashimura, Macromolecules 28 (1995) 1721.
[118] G. Moineau, C. Granel, P. Dubois, R. Jerome, P. Teyssie, Macromolecules 31 (1998) 542.
[119] C. Granel, P. Dubois, R. Jerome, P. Teyssie, Macromolecules 29 (1996) 8576.
[120] P. Lecomte, I. Drapier, P. Dubois, P. Teyssie, R. Jerome, Macromolecules 30 (1997) 7631.
[121] D.M. Haddleton, C.B. Jasieczek, M.J. Hannon, A.J. Shooter, Macromolecules 30 (1997) 2190.
[122] J.-S. Wang, K. Matyjaszewski, Macromolecules 28 (1995) 7901.
[123] K.A. Davis, K. Matyjaszewski, J. Macromol. Sci., Pure Appl. Chem. A 41 (2004) 449.
[124] B. Gobelt, K. Matyjaszewski, Macromol. Chem. Phys. 201 (2000) 1619.
[125] J. Gromada, J. Spanswick, K. Matyjaszewski, Macromol. Chem. Phys. 205 (2004) 551.
[126] S.C. Hong, K. Matyjaszewski, Macromolecules 35 (2002) 7592.
[127] P. Kubisa, Prog. Polym. Sci. 29 (2004) 3.
[128] T. Sarbu, K. Matyjaszewski, Macromol. Chem. Phys. 202 (2001) 3379.
[129] J. Xia, T. Johnson, S.G. Gaynor, K. Matyjaszewski, J. DeSimone, Macromolecules 32 (1999) 4802.
[130] J. Xia, K. Matyjaszewski, Macromolecules 32 (1999) 2434.
[131] J. Xia, X. Zhang, K. Matyjaszewski, ACS Symp. Ser. 760 (2000) 207.
[132] T. Nishikawa, M. Kamigaito, M. Sawamoto, Macromolecules 32 (1999) 2204.
[133] T. Ando, M. Kamigaito, M. Sawamoto, Tetrahedron 53 (1997) 15445.
[134] K. Matyjaszewski, Polym. Int. 52 (2003) 1559.
[135] S.S. Sheiko, S.A. Prokhorova, K.L. Beers, K. Matyjaszewski, I.I. Potemkin, A.R. Khokhlov, M. Moeller, Macromolecules 34 (2001) 8354.
[136] V. Percec, B. Barboiu, Macromolecules 28 (1995) 7970.
[137] T. Grimaud, K. Matyjaszewski, Macromolecules 30 (1997) 2216.
[138] V. Percec, B. Barboiu, H.-J. Kim, J. Am. Chem. Soc. 120 (1998) 305.

[139] M. Destarac, J.M. Bessiere, B. Boutevin, Macromol. Rapid Commun. 18 (1997) 967.
[140] J. Xia, K. Matyjaszewski, Macromolecules 30 (1997) 7697.
[141] X. Zhang, J. Xia, K. Matyjaszewski, Macromolecules 1998 (1998) 5167.
[142] G. Kickelbick, K. Matyjaszewski, Macromol. Rapid Commun. 20 (1999) 341.
[143] J. Xia, X. Zhang, K. Matyjaszewski, in: B.M. Novak (Ed.), Transition Metal Catalysis in Macromolecular Design, American Chemical Society, Washington, DC, 2000, p. 207.
[144] J. Xia, K. Matyjaszewski, Macromolecules 32 (1999) 2434.
[145] J. Xia, S.G. Gaynor, K. Matyjaszewski, Macromolecules 31 (1998) 5958.
[146] W.E. Hatfield, R. Whyman, Transition Met. Chem. 5 (1969) 47.
[147] F.H. Jardin, Adv. Inorg. Chem. Radiochem. 17 (1975) 115.
[148] K.D. Karlin, J.A. Zubieta, Copper Coordination Chemistry: Biochemical and Inorganic Perspectives, Adenine Press, New York, 1983.
[149] G. Wilkinson, Comprehensive Coordination Chemistry, Pergamon Press, New York, 1987.
[150] M. Munakata, S. Kitagawa, A. Asahara, H. Masuda, Bull. Chem. Soc. Jpn. 60 (1987) 1927.
[151] J. Foley, S. Tyagi, B.J. Hathaway, J. Chem. Soc., Dalton Trans. (1984) 1.
[152] B.W. Skelton, A.F. Waters, A.H. White, Aust. J. Chem. 44 (1991) 1207.
[153] R.D. Willett, G. Pon, C. Nagy, Inorg. Chem. 40 (2001) 4342.
[154] P.J. Burke, D.R. McMillin, W.R. Robinson, Inorg. Chem. 19 (1980) 1211.
[155] A.T. Levy, M.M. Olmstead, T.E. Patten, Inorg. Chem. 39 (2000) 1628.
[156] K.V. Goodwin, D.R. McMillin, W.R. Robinson, Inorg. Chem. 25 (1986) 2033.
[157] J.F. Dobson, B.E. Green, P.C. Healy, C.H.L. Kennard, C. Pukawatchai, A.H. White, Inorg. Chem. 37 (1984) 649.
[158] B.R. James, R.J.P. Williams, J. Chem. Soc. (1961) 2007.
[159] M. Asplund, S. Jagner, M. Nilsson, Acta Chem. Scand. A 37 (1983) 57.
[160] S. Anderson, S. Jagner, Acta Chem. Scand. A 39 (1985) 297.
[161] G.A. Bowmaker, L.D. Brockliss, R. Whiting, Aust. J. Chem. 26 (1973) 29.
[162] J.A. Creighton, E.R. Lippincott, J. Chem. Soc. (1963) 5134.
[163] D.N. Waters, B. Basak, J. Chem. Soc. A (1971) 2733.
[164] J. Gobernado, J. Aroca, A. Desaya, Spectrochim. Acta 50A (1994) 1243.
[165] T. Kobayashi, Spectrochim. Acta 26A (1970) 1313.
[166] A.T. Kowal, J. Skarzewski, Spectrochim. Acta 41A (1985) 563.
[167] R. Batistuzzi, G. Peyronel, Spectrochim. Acta 36A (1980) 511.
[168] J.A. Real, J. Borras, X. Solans, M. Font-Altaba, Transition Met. Chem. 12 (1987) 79.
[169] M.M. Campos-Valletter, K. Figueroa, R.O. Latorre, G. Diaz, J. Costamagna, J.C. Canales, M. Rey-Lafon, J. Deroault, Vibr. Spectrosc. 6 (1993) 25.
[170] R.M. Everly, D.R. McMillin, J. Phys. Chem. 95 (1991) 9071.
[171] H. Irving, R.J.P. Williams, J. Chem. Soc. (1953) 319.
[172] P. Day, N. Sanders, J. Chem. Soc. A (1967) 1536.
[173] A.K. Ichinaga, J.R. Kirchhoff, D.R. McMillin, C.O. Dietrich-Buchecker, P.A. Marnot, J.P. Sauvage, Inorg. Chem. 26 (1987) 4290.
[174] C. Daul, C.W. Schlapfer, A. Goursot, E. Peningault, J. Weber, Chem. Phys. Lett. 78 (1981) 304.
[175] W.L. Parker, G.A. Crosby, J. Phys. Chem. 93 (1989) 5692.
[176] S. Kitagawa, M. Munakata, Inorg. Chem. 20 (1981) 2261.
[177] V. Katta, S.K. Chowdhury, B.T. Chait, J. Am. Chem. Soc. 112 (1990) 5348.
[178] R. Colton, B.D. James, I.D. Potter, J.C. Traeger, Inorg. Chem. 32 (1993) 2626.
[179] S.R. Wilson, Y. Wu, Organometallics 12 (1993) 1478.
[180] B.H. Lipshutz, K.L. Stevens, B. James, J.G. Pavlovich, J. Am. Chem. Soc. 118 (1996) 6796.
[181] B.H. Lipshutz, J. Keith, D.J. Buzard, Organometallics 18 (1999) 1571.
[182] S.R. Wilson, A. Yasmin, Y. Wu, J. Org. Chem. 57 (1992) 6941.
[183] T. Pintauer, C.B. Jasieczek, K. Matyjaszewski, J. Mass Spectrom. 35 (2000) 1295.
[184] R.L. Kronig, Z. Phys. 70 (1931) 317.
[185] R.L. Kronig, Z. Phys. 75 (1932) 468.
[186] R.L. Kronig, Z. Phys. 75 (1932) 191.
[187] E.A. Stern, Phys. Rev. B 10 (1974) 3027.
[188] B.M. Kincaid, P. Eisenberger, Phys. Rev. Lett. 34 (1975) 1361.
[189] R.E. Watson, M.L. Perlman, Science 199 (1978) 157.
[190] B.W. Batterman, N.W. Ashcroft, Science 206 (1979) 157.
[191] P.A. Lee, P. Citrin, P. Eisenberger, B.M. Kincaid, Rev. Mod. Phys. 53 (1980) 769.
[192] B.K. Teo, Acc. Chem. Res. 13 (1980) 412.
[193] T. Pintauer, U. Reinohl, M. Feth, H. Bertagnolli, K. Matyjaszewski, Eur. J. Inorg. Chem. 11 (2003) 2082.
[194] T. Pintauer, U. Reinohl, M. Feth, H. Bertagnolli, K. Matyjaszewski, Polym. Prepr. (Am. Chem. Soc., Div. Polym. Chem.) 43 (2) (2002) 219.
[195] G. Kickelbick, U. Reinohl, T.S. Ertel, A. Weber, H. Bertagnolli, K. Matyjaszewski, Inorg. Chem. 40 (2001) 6.
[196] H. Masuda, K. Machida, J. Chem. Soc., Dalton Trans. (1988) 1907.
[197] J.E. Penner-Hahn, Coord. Chem. Rev. 190–192 (1999) 1101.
[198] M. Munakata, S. Kitagawa, S. Kosome, A. Asahara, Inorg. Chem. 25 (1986) 2622.
[199] R. Jones, Chem. Rev. 68 (1968) 785.
[200] D.M. Haddleton, M.C. Crossman, K.H. Hunt, Macromolecules 30 (1997) 3992.
[201] D.M. Haddleton, D.J. Duncalf, D. Kukulj, M.C. Crossman, S.G. Jackson, S.A.F. Bon, A.J. Clark, A.J. Schooter, Eur. J. Inorg. Chem. (1998) 1799.
[202] F. Lecolley, C. Waterson, A.J. Carmichael, G. Mantovani, S. Harrison, H. Chappell, A. Limer, P. Williams, K. Ohno, D.M. Haddleton, J. Mater. Chem. 13 (2003) 2689.
[203] J. Lad, S. Harrison, G. Mantovani, D.M. Haddleton, Dalton Trans. (2003) 4175.
[204] J. Lad, S. Harrison, D.M. Haddleton, ACS Symp. Ser. 854 (2003) 148.
[205] S. Perrier, D. Berthier, I. Willoughby, D. Batt-Coutrot, D.M. Haddleton, Macromolecules 35 (2002) 2941.
[206] S. Perrier, S.P. Armes, X.S. Wang, F. Malet, D.M. Haddleton, J. Polym. Sci., Part A: Polym. Chem. 39 (2001) 1696.
[207] A.J. Clark, G.M. Battle, A.M. Heming, D.M. Haddleton, A. Bridge, Tetrahedron Lett. 42 (2001) 2003.
[208] D.M. Haddleton, M.C. Crossman, C. Martin, B.H. Dana, D.J. Duncalf, A.M. Heming, D. Kukulj, A.J. Shooter, Macromolecules 32 (1999) 2110.
[209] H. Zhang, B. Klumperman, W. Ming, H. Fischer, R. Linde, Macromolecules 34 (2001) 6169.
[210] M. Pasquali, C. Floriani, G. Venturi, A. Gaetani-Manfredotti, A. Chiesi-Villa, J. Am. Chem. Soc. 104 (1982) 4092.
[211] L.M. Engelhardth, R.I. Papasergio, A.H. White, Aust. J. Chem. 37 (1984) 2207.
[212] M.F. Garbauskas, D.A. Haitko, J.S. Kasper, J. Crystallogr. Spectrosc. Res. 16 (1986) 729.
[213] J. Xia, K. Matyjaszewski, Macromolecules 32 (1999) 2434.
[214] M. Pasquali, F. Marchetti, C. Floriani, Inorg. Chem. 17 (1978) 1684.
[215] M.I. Bruce, J. Organomet. Chem. 44 (1972) 209.
[216] T. Ogura, Inorg. Chem. 15 (1976) 2301.
[217] E. Kimura, T. Koike, M. Kodama, D. Meyerstein, Inorg. Chem. 28 (1989) 2998.

[218] M. Pasquali, C. Floriani, A. Gaetani-Manfredotti, A. Chiesi-Villa, Inorg. Chem. 18 (1979) 3535.
[219] M. Pasquali, F. Marchetti, C. Floriani, Inorg. Chem. 17 (1978) 1684.
[220] L.E. Sutton, Tables of Interatomic Distances and Configurations in Molecules and Ions, The Chemical Society, London, 1965.
[221] W. Braunecker, T. Pintauer, N.V. Tsarevsky, G. Kickelbick, K. Matyjaszewski, J. Organomet. Chem., in press.
[222] T. Pintauer, N.V. Tsarevsky, G. Kickelbick, K. Matyjaszewski, Polym. Prepr. (Am. Chem. Soc., Div. Polym. Chem.) 43 (2) (2002) 221.
[223] G. Wilkinson, Comprehensive Coordination Chemistry, Pergamon Press, New York, 1987.
[224] M. Satterfield, J.S. Brodbelt, Inorg. Chem. 40 (2001) 5393.
[225] R.R. Gagne, J.L. Allison, C.A. Koval, W.S. Mialki, T.J. Smith, R.A. Walton, J. Am. Chem. Soc. 102 (1980) 1095.
[226] M. Costas, A. Llobet, J. Mol. Catal. A 142 (1999) 113.
[227] M. Munakata, N. Shigeru, S. Hiromasa, J. Chem. Soc., Chem. Commun. 5 (1980) 219.
[228] J. Gromada, K. Matyjaszewski, Macromolecules 35 (2002) 6167.
[229] M. Becker, F.W. Heinemann, S. Schindler, Chem. Eur. J. 5 (1999) 3124.
[230] M. Becker, F.W. Heinemann, F. Knoch, W. Donaubauer, G. Liehr, S. Schindler, G. Golub, H. Cohen, D. Meyerstein, Eur. J. Inorg. Chem. (2000) 719.
[231] F. Thaler, C.D. Hubbard, F.W. Heinemann, R. Eldik, S. Schindler, I. Fabian, A.M. Dittler-Klingemann, F.E. Hahn, C. Orvig, Inorg. Chem. 37 (1998) 4022.
[232] Z.-L. Lu, M.S.A. Hamza, R. Eldik, Eur. J. Inorg. Chem. (2001) 503.
[233] J.H. Coates, P.R. Collins, S.F. Lincoln, Aust. J. Chem. 33 (1980) 1381.
[234] J.H. Coates, P.R. Collins, S.F. Lincoln, J. Chem. Soc., Faraday Trans. 75 (1979) 1236.
[235] P.C. Healy, L.M. Engelhardt, V.A. Patrick, A.H. White, J. Chem. Soc., Dalton Trans. (1985) 2541.
[236] M. Pasquali, C. Floriani, G. Venturi, A.G. Mandredotti, A. Chiesi-Villa, J. Am. Chem. Soc. 104 (1982) 4092.
[237] L.M. Engelhardt, R.A. Papsergio, A.H. White, Aust. J. Chem. 37 (1984) 2207.
[238] F. Schon, M. Hartenstein, A.H.E. Muller, Macromolecules 34 (2001) 5394.
[239] M. Bednarek, T. Biedron, P. Kubisa, Macromol. Chem. Phys. 201 (2000) 58.
[240] B.J. Hathaway, D.E. Billing, Acta Crystallogr., Sect. B 35 (1979) 2910.
[241] M.J. Heeg, J.F. Endicott, M.D. Glick, M.A. Khalifa, Acta Crystallogr., Sect. B 38 (1982) 730.
[242] J. Foley, D. Kennefick, D. Phelan, S. Tyagi, B.J. Hathaway, J. Chem. Soc., Dalton Trans. (1983) 2333.
[243] H. Nakai, Bull. Chem. Soc. Jpn. 44 (1971) 2412.
[244] O.P. Anderson, J. Chem. Soc., Dalton Trans. (1972) 2597.
[245] M.A. Khan, D.G. Tuck, Acta Crystallogr., Sect. B 37 (1981) 1409.
[246] S. Tyagi, B.J. Hathaway, S. Kramer, H. Stratemeier, D. Reinen, J. Chem. Soc., Dalton Trans. (1984) 2087.
[247] F.S. Stephens, P.A. Tucker, J. Chem. Soc., Dalton Trans. (1973) 2293.
[248] W.D. Harrison, D.M. Kennedy, N.J. Ray, R. Sheahan, B.J. Hathaway, J. Chem. Soc., Dalton Trans. (1981) 1556.
[249] J. Kaiser, G. Brauer, F.A. Schroeder, I.F. Taylor, S.E. Rasmussen, J. Chem. Soc., Dalton Trans. (1974) 1490.
[250] P. Nagle, C. O'Sullivan, B.J. Hathaway, E. Muller, J. Chem. Soc., Dalton Trans. (1990) 3399.
[251] C. O'Sullivan, G. Murphy, B. Murphy, B. Hathaway, J. Chem. Soc., Dalton Trans. 11 (1999) 1835.
[252] B.J. Hathaway, B. Murphy, Acta Crystallogr., Sect. B 36 (1980) 295.
[253] T. Pintauer, J. Qiu, G. Kickelbick, K. Matyjaszewski, Inorg. Chem. 40 (2001) 2818.
[254] G. Kickelbick, T. Pintauer, K. Matyjaszewski, New J. Chem. 26 (2002) 462.
[255] G.A. Barclay, B.F. Hoskins, C.H.L. Kennard, J. Chem. Soc. (1963) 5691.
[256] A.W. Addison, T. Nageswara Rao, J. Reedijk, J. van Rijn, G.C. Verschoor, J. Chem. Soc., Dalton Trans. (1984) 1349.
[257] G. Murphy, C. O'Sullivan, B. Murphy, B.J. Hathaway, Inorg. Chem. 37 (1998) 240.
[258] G. Murphy, P. Nagle, B. Murphy, B.J. Hathaway, J. Chem. Soc., Dalton Trans. (1997) 2645.
[259] R.P. Hammond, M. Cavaluzzi, R.C. Haushalter, J.A. Zubieta, Inorg. Chem. 38 (1999) 1288.
[260] R.D. Willet, Chem. Coord. Rev. 109 (1991) 181.
[261] S. Ishiguro, L. Nagy, H. Ohtaki, Bull. Chem. Soc. Jpn. 60 (1987) 1053.
[262] R. Griesser, H. Sigel, Inorg. Chem. 10 (1971) 2229.
[263] R. Peter, R. Huber, R. Griesser, H. Sigel, Inorg. Chem. 10 (1971) 945.
[264] Y. Abe, G. Wada, Bull. Chem. Soc. Jpn. 54 (1981) 3334.
[265] W.A.E. McBryde, A Critical Review of Equilibrium Data for Proton and Metal Complexes of 1,10-Phenanthroline, 2,2′-Bipyridine and Related Compounds, IUPAC Chemical Data Series, Pergamon Press, 1978.
[266] Y. Abe, G. Wada, Bull. Chem. Soc. Jpn. 60 (1987) 1936.
[267] J.N. Butler, Ionic Equilibrium: A Mathematical Approach, Addison-Wesley, Reading, MA, 1964.
[268] M.A. Khan, J. Meullemeestre, M.J. Schwing, F. Vierling, Inorg. Chem. 28 (1989) 3306.
[269] J.C. Barnes, D.N. Hume, Inorg. Chem. 2 (1963) 444.
[270] M.R. Sundberg, R. Kivekas, J. Ruiz, J.M. Moreno, E. Colacio, Inorg. Chem. 31 (1992) 1062.
[271] P.S. Braterman, Inorg. Chem. 2 (1963) 448.
[272] S. Ishiguro, K. Ozutsumi, L. Nagy, H. Ohtaki, Bull. Chem. Soc. Jpn. 60 (1998) 1691.
[273] S.E. Manahan, R.T. Iwamoto, Inorg. Chem. 4 (1965) 1409.
[274] M.A. Hiskey, R.R. Ruminski, Inorg. Chim. Acta 112 (1986) 189.
[275] G.A. McLachlan, G.D. Fallon, R.L. Martin, L. Spiccia, Inorg. Chem. 34 (1995) 254.
[276] B.J. Hathaway, Comprehensive Coordination Chemistry, Pergamon Press, Oxford, England, 1987.
[277] J. Ferguson, Prog. Inorg. Chem. 12 (1970) 159.
[278] N.S. Hush, R.J.M. Hobbs, Prog. Inorg. Chem. 10 (1968) 259.
[279] E.J. Solomon, K.W. Penfield, D.E. Wilcox, Struct. Bonding (Berlin) 53 (1983) 1.
[280] I.S. Ahuja, S. Tripathi, Spectrochim. Acta 48A (1992) 759.
[281] M. Brierley, W.J. Geary, J. Chem. Soc. A (1967) 963.
[282] M. Brierley, W.J. Geary, J. Chem. Soc. A (1968) 1641.
[283] N. Ray, S. Tyagi, B. Hathaway, J. Chem. Soc., Dalton Trans. (1982) 143.
[284] D.E. Billing, A.E. Underhill, D.M. Adams, D.M. Morris, J. Chem. Soc. A (1966) 902.
[285] W.J. Geary, J. Chem. Soc. A (1969) 71.
[286] P.S. Braterman, Inorg. Chem. 2 (1963) 448.
[287] B.J. Hathaway, D.E. Billing, Coord. Chem. Rev. 5 (1970) 143.
[288] H.H. Perkampus, UV–Vis Spectroscopy and its Applications, Springer-Verlag, Berlin, 1992.
[289] R.S. Drago, Physical Methods for Chemists, Saunders College Pub., Ft. Worth, 1992.
[290] V. Balzani, V. Carassity, Photochemistry of Coordination Compounds, Academic Press, New York, 1970.
[291] S.K. Weit, G. Ferraudi, P.A. Grutsch, C. Kutal, Coord. Chem. Rev. 128 (1993) 225.
[292] G. Murphy, C. O'Sullivan, B. Murphy, B. Hathaway, Inorg. Chem. 37 (1998) 240.
[293] J. Xia, K. Matyjaszewski, Macromolecules 30 (1997) 7692.

[294] B. Hathaway, M. Duggan, A. Murphy, J. Mullande, C. Power, A. Walsh, B. Walsh, Coord. Chem. Rev. 36 (1981) 267.
[295] I. Bertini, D. Gatteschi, A. Scozzafava, Coord. Chem. Rev. 29 (1979) 67.
[296] B. Hathaway, D.E. Billing, Coord. Chem. Rev. 5 (1970) 143.
[297] B. Knuehl, T. Pintauer, A. Kajiwara, H. Fischer, K. Matyjaszewski, Macromolecules 36 (2003) 8291.
[298] A. Kajiwara, K. Matyjaszewski, M. Kamachi, Macromolecules 31 (1998) 5695.
[299] A. Kajiwara, K. Matyjaszewski, Macromol. Rapid Commun. 19 (1998) 319.
[300] A. Kajiwara, K. Matyjaszewski, Polym. J. 31 (1999) 70.
[301] S.R. Breeze, S. Wang, Inorg. Chem. 35 (1996) 3404.
[302] E.L. Muetterties, J.L. Guggenberger, J. Am. Chem. Soc. 96 (1974) 1748.
[303] M.J. Scott, R.H. Holm, J. Am. Chem. Soc. 116 (1994) 11357.
[304] S.J. Barlow, S.J. Hill, J.E. Hocking, P. Hubberstey, W.-S. Li, J. Chem. Soc., Dalton Trans. 24 (1997) 4701.
[305] F.R. Hartley, Chem. Rev. 73 (1973) 163.
[306] D.K. Towle, S.K. Hoffmann, W.E. Hatfield, P. Singh, P. Chaudhuri, K. Weighardt, Inorg. Chem. 24 (1985) 4393.
[307] D.K. Towle, W.E. Hatfield, K. Weighardt, C. Phalguni, J. Weiss, Mol. Cryst. Liq. Cryst. 107 (1984) 161.
[308] M.K. Urtiaga, M.I. Arriortua, R. Cortes, T. Rojo, Acta Crystallogr. C 52 (1996) 3007.
[309] C. Feng, D. Cheng, D. Xu, Y. Zhen, J. Lin, Y. Xu, J. Coord. Chem. 51 (2000) 67.
[310] S. Liu, C. Su, Polyhedron 151 (1996) 1141.
[311] M.I. Arriortua, J.L. Mesa, T. Rojo, T. Debaerdemaeker, D. Beltran-Porter, H. Stratemeier, D. Reinen, Inorg. Chem. 27 (1988) 2976.
[312] T. Rojo, M. Vlasse, D. Beltran-Porter, Acta Crystallogr. C 39 (1983) 194.
[313] J. Emsley, M. Arif, Inorg. Chim. Acta 143 (1988) 25.
[314] J. Via, M.I. Arriortua, T. Rojo, J.L. Mesa, A. Garcia, Bull. Soc. Chim. Belg. 98 (1989) 179.
[315] R. Cortes, L. Lezama, J.I.R. Larramendi, M. Insausti, J.V. Faldago, G. Madariaga, T. Rojo, J. Chem. Soc., Dalton Trans. (1994) 2573.
[316] R. Cortes, M.K. Urtiaga, L. Lezama, J.I.R. Larramendi, M.I. Arriortua, T. Rojo, J. Chem. Soc., Dalton Trans. (1993) 3685.
[317] M. Rodriguez, A. Llobet, M. Corbella, Polyhedron 19 (2000) 2483.
[318] T. Rojo, M.I. Arriortua, J. Ruiz, J. Darriet, G. Villeneuve, D. Beltran-Porter, J. Chem. Soc., Dalton Trans. 2 (1987) 285.
[319] T. Rojo, M.I. Arriortua, J.L. Mesa, R. Cortes, G. Villeneuve, D. Beltran-Porter, Inorg. Chim. Acta 134 (1987) 59.
[320] J.V. Folgado, W. Henke, R. Allmann, H. Stratemeier, D. Beltran-Porter, T. Rojo, D. Reinen, Inorg. Chem. 29 (1990) 2035.
[321] M.I. Arriortua, T. Rojo, J.M. Amigo, G. Germain, J.P. Declerco, Acta Crystallogr. B 38 (1982) 1323.
[322] M.D. Vaira, P.L. Orioli, Acta Crystallogr. B 24 (1968) 595.
[323] P.C. Jain, E.C. Lingafelter, J. Am. Chem. Soc. 89 (1967) 6131.
[324] M. Duggan, N.J. Ray, B. Hathaway, G. Tomlinson, P. Brint, K. Pelin, J. Chem. Soc., Dalton Trans. (1984) 1342.
[325] B. Bosnich, M.L. Tobe, G.A. Webb, Inorg. Chem. 4 (1965) 1109.
[326] R.L. Webb, M.L. Mino, E.L. Blinn, A.A. Pinkerton, Inorg. Chem. 32 (1993) 1396.
[327] M.C. Syka, R.C. Smierciak, E.L. Blinn, R.E. DeSimone, J.V. Passariello, Inorg. Chem. 17 (1978) 82.
[328] A.W. Addison, E. Sinn, Inorg. Chem. 22 (1983) 1225.
[329] K. Matyjaszewski, J. Qiu, N.V. Tsarevsky, B. Charleux, J. Polym. Sci., Part A: Polym. Chem. 38 (2000) 4724.
[330] K. Matyjaszewski, H.-J. Paik, P. Zhou, S.J. Diamanti, Macromolecules 34 (2001) 5125.
[331] K. Matyjaszewski, B. Gobelt, H.-J. Paik, C.P. Horwitz, Macromolecules 34 (2001) 430.
[332] A.K. Nanda, K. Matyjaszewski, Macromolecules 36 (2003) 8222.
[333] A.K. Nanda, K. Matyjaszewski, Macromolecules 36 (2003) 599.
[334] A.K. Nanda, K. Matyjaszewski, Macromolecules 36 (2003) 1487.
[335] T. Pintauer, W. Braunecker, E. Collange, R. Poli, K. Matyjaszewski, Macromolecules 37 (2004) 2679.